Genomics and Proteomics:

Structural Basis for Phosphorylation and Lysine Acetylation Crosstalk in a Kinase Motif Associated with Myocardial Ischemia and Cardioprotection

Benjamin L. Parker, Nicholas E. Shepherd, Sophie Trefely, Nolan J. Hoffman, Melanie Y. White, Kasper Engholm-Keller, Brett D. Hambly, Martin R. Larsen, David E. James and Stuart J. Cordwell

J. Biol. Chem. published online July 9, 2014

JBC Papers in Press. Published on July 9, 2014 as Manuscript M114.556035
The latest version is at http://www.jbc.org/cgi/doi/10.1074/jbc.M114.556035

Structural basis for phosphorylation and lysine acetylation crosstalk in a kinase motif associated with myocardial ischemia and cardioprotection

Benjamin L. Parker [1,2,3], Nicholas E. Shepherd [4], Sophie Trefely [2], Nolan J. Hoffman [2,3], Melanie Y. White [4,5], Kasper Engholm-Keller [5], Brett D. Hambly [1,5], Martin R. Larsen [6], David E. James [2,3,5], Stuart J. Cordwell [1,4,5*]

[1] Discipline of Pathology, School of Medical Sciences, The University of Sydney, Australia 2006.

[2] Diabetes and Obesity Program, and [3] Biological Mass Spectrometry Unit, Garvan Institute of Medical Research, Australia 2010

[4] School of Molecular Bioscience, The University of Sydney, Australia, 2006.

[5] Charles Perkins Centre, The University of Sydney, Australia, 2006

[6] Department of Biochemistry and Molecular Biology, University of Southern Denmark, Campusvej 55, 5230 Odense M, Denmark

***Corresponding Author:** Associate Professor Stuart J. Cordwell, Charles Perkins Centre, The Hub Building D17, The University of Sydney, Australia, 2006. Phone: (61-2) 9351-6050; Fax: (61-2) 9351-4726; E-mail: stuart.cordwell@sydney.edu.au

Running Title: PTM crosstalk during ischemia and cardioprotection

Keywords: myocardial ischemia / cardioprotection / phosphorylation / lysine acetylation / post-translational modification

Background: Myocardial ischemia and cardioprotection induce signal networks mediated by post-translational modification.
Results: Phosphorylation sites altered by ischemia and/or cardioprotection were influenced by inhibition of lysine acetylation consistent with crosstalk.
Conclusion: Lysine acetylation induces proximal dephosphorylation in a kinase motif by salt-bridge inhibition.
Significance: Crosstalk is likely to be an important aspect of signalling during ischemia and cardioprotection.

Abstract

Myocardial ischemia and cardioprotection by ischemic pre-conditioning (IPC) induce signal networks aimed at survival, or cell death if the ischemic period is prolonged. These pathways are mediated by protein post-translational modifications (PTM) that are hypothesized to crosstalk with and regulate each other. Phosphopeptides and lysine acetylated peptides were quantified in isolated rat hearts subjected to ischemia or IPC, with and without splitomicin inhibition of lysine deacetylation. We show lysine acetylation (AcetylK)-dependent activation of AMPK, AKT and PKA kinases during ischemia. Phosphorylation and AcetylK sites mapped onto tertiary structures were proximal in >50% of proteins investigated, yet were mutually exclusive in 50 IPC- and / or ischemia-associated peptides containing the KxxS basophilic protein kinase consensus motif. Modifications in this motif were modelled in the *C*-terminus of muscle-type creatine kinase (CKM). AcetylK increased proximal dephosphorylation by 10-fold. Structural analysis of modified CKM peptide variants by 2D-NMR revealed stabilization *via* a lysine-phosphate salt bridge, which was disrupted by AcetylK resulting in backbone flexibility and increased phosphatase accesibility.

Introduction

Prolonged blockage of coronary blood flow (ischemia), even with subsequent restoration (reperfusion), may result in cardiomyocyte apoptosis and necrosis. Ischemia / reperfusion

(I/R) thus represents a significant clinical burden. Ischemic pre-conditioning (IPC), a series of short I/R cycles prior to extended ischemia, elicits a degree of cardioprotection against I/R injury. The oxygen supply / demand imbalance upon ischemia reduces oxidative metabolism and results in depletion of intracellular ATP accompanied by a time-dependent rise in AMP. Anaerobiosis also generates pyruvate conversion to lactate to maintain oxidized NAD^+ levels, which leads to intracellular acidosis and promotes Na^+ and Ca^{2+} overload (1,2). Activation of signal pathways in ischemia and IPC is established (3,4) and include mitogen-activated protein kinases (MAPKs) (5), protein kinase C (PKC) (6-8), phosphatidyl inositol 3'-hydroxy kinase/AKT complex (PI3K/AKT) (9), and cyclic AMP-dependent protein kinase A (PKA) (10-11).

The ischemia-associated increase in AMP:ATP also activates a network initiated in part by AMP-activated protein kinase (AMPK). AMPK regulates fatty acid metabolism, where AMPK-mediated phosphorylation inactivates acetyl-CoA carboxylase (ACC) resulting in a decrease in cytosolic malonyl-CoA (12) and an increase in fatty acid uptake and oxidation in the mitochondria (13-15). AMPK activation also modulates energy consumption (16), cell survival and regulation of the fuel-sensing sirtuin (SIRT) family of protein deacetylases (17). AMPK and SIRT1 regulate each other, which suggests an AMPK / SIRT1 sensing cycle with phosphorylation / acetylation crosstalk on common substrates (18). The SIRTs are a family of 7 NAD^+-dependent enzymes whose activity is influenced by cellular energy and redox status (19). SIRT1 over-expression confers myocardial protection during oxidative stress (20) and prevents apoptosis *via* p53 inactivation (21), while splitomicin-mediated inhibition of SIRT1 attenuates IPC (22), which collectively provides strong evidence that lysine acetylation (AcetylK) / deacetylation contributes to cardioprotection and cell survival during ischemia.

Post-translational modification (PTM) crosstalk is best exemplified in the 'chromatin code' (23-26). Crosstalk can include: i) competitive modification of the same site; ii) modification influencing additional PTM at a proximal site; or iii) a PTM activating / deactivating the modifying enzyme for a second modification. Studies of histone PTM crosstalk identified a modification that subsequently resulted in the alteration of a secondary *cis* (intra-molecular) modification - phosphorylation of S10 on histone H3 increases acetylation of K14 (27-28). This process was also observed at a *trans* (inter-molecular) level - ubiquitylation of histone H2B stimulates histone H3 methylation (29). Crosstalk can also influence PTM kinetics (30-33). Alternatively, PTMs may activate / deactivate modifying enzymes, including (de)acetylation of kinases (34-37), for example SIRT1 promotion of AKT activity (38), (de)phosphorylation of deacetylases / acetyltransferases (39-42), or a PTM-modifying enzyme regulating global levels of another PTM (43-44). Crosstalk between phosphorylation and AcetylK can include the recruitment of kinases / phosphatases by AcetylK (45-46), the recruitment of histone deacetylases (HDACs) / acetyltransferases by phosphorylation (47-49), or where either phosphorylation or AcetylK are required for the other to occur at a proximal site (50). Examples of site-specific competition include between acetylation and phosphorylation of serine in the activation loop of MAP2K6 (51); and *O*-Glc*N*Acylation and phosphorylation of T58 in c-Myc (52); S1177 in endothelial nitric oxide synthase (53); and S733 in IKKβ (54).

Peptide-centric enrichment combined with quantitative tandem mass spectrometry (MS/MS) has become the gold standard for generating global phosphopeptide profiles under a variety of stimuli and disease states (55-57), while antibody-based enrichment of acetylated peptides followed by MS/MS has also proven successful (58-63). We utilized sequential enrichment to globally quantify phosphorylated and lysine acetylated peptides in isolated rat hearts subjected to ischemia and IPC, in the presence or absence of splitomicin inhibition of lysine deacetylation, using isobaric labeling and MS/MS. These data enabled an evaluation of sequence motifs displaying evidence of PTM crosstalk, which showed that phosphorylation and AcetylK are mutually exclusive in 50 ischemia / IPC regulated peptides containing a basophilic protein kinase motif (KxxS). We determined the rates of crosstalk between PTM in the *C*-terminal region of muscle-type creatine kinase (CKM) and demonstrated the formation of a phosphate - lysine salt bridge. AcetylK disrupts the phosphate - lysine

interaction and results in increased de-phosphorylation at this site.

Experimental Procedures

Rat heart isolation. Male Lewis rats (approximately 200 g) were euthanized with an intraperitoneal injection of sodium pentobarbital (0.5 mg/g; University of Sydney Animal Ethics Committee approval K20/6-2009/3/5078). The aorta was cut ~1 cm above the aortic valve, the heart removed and placed in ice-cold saline solution (0.9% (w/v) NaCl, pH 7.4). Hearts were subjected to Langendorff perfusion using oxygenated Krebs-Henseleit buffer (118mM NaCl, 25mM $NaHCO_3$, 1.2mM KH_2PO_4, 4.8mM KCl, 1.2mM $MgSO_4$, 11mM glucose, 2.0mM $CaCl_2$, pH 7.4) at 37°C, as described (64). Heart rates and left ventricular developed pressure (LVDP) were recorded (LabChart, ADInstuments, Bella Vista, Australia) and measured as a rate pressure product (RPP; beats / min x LVDP in mmHg). For ischemia and IPC, hearts were equilibrated for a baseline period of 15 mins with normoxic perfusion and then assigned to 12 groups: i) 0 min; ii) 2 min; iii) 10 min, iv) 20 min of no-flow ischemia (n=3 for each time point); v) 0 min; vi) 2 min; vii) 10 min; viii) 20 min of no-flow ischemia following 15 min equilibration with 10μM splitomicin (n=3 for each time point); ix) acute IPC with 3 x 2 min cycles of I/R (n=3); x) acute IPC with 3 x 2 min I/R following 15 min equilibration with 10μM splitomicin (n=3); xi) 20 min of normoxic perfusion (n=3); and xii) 20 min of normoxic perfusion with 10μM splitomicin. Hearts were snap frozen and stored at -80°C. All hearts achieved a RPP of 25,000 (+/-5000), a flow rate of 9 mL/min and a perfusion pressure of 80 mmHg at the end of the baseline period. Myocardial function was determined by comparing the RPP for additional hearts subjected to 20 min ischemia, followed by 30 min reperfusion, to allow determination of functional recovery. The extent of necrosis was determined by staining hearts with triphenyltetrazolium chloride (TTC) (64). Following normoxic perfusion, no significant difference in the functional performance of the hearts was observed (RPP = 92.2% of baseline; Figure S1). Hearts subjected to 20 min ischemia and 30 min reperfusion showed loss of hemodynamic performance (RPP = ~30% of baseline; *p*-value <0.05) and evidence of necrosis (17.8% ± 3.6% negative TTC staining of LV mass compared with 0.4% ± 0.1% for baseline hearts) (Figure S1). Splitomicin had no significant effect on normoxic heart function, as reported (22).

Cell culture. Rat L6 myoblasts were 2-plex SILAC labelled in alpha-MEM containing 5.5mM glucose (Life Technologies, Gaithersburg MD) and 10% fetal bovine serum (Hyclone, Logan UT). Following 5 passages, cells at 80% confluence were transfected with lipofectamine-2000 and 15 μg plasmid DNA. The plasmid consisted of human CKM cloned into a pCMV5 plasmid containing an *N*-terminal FLAG tag and was generously provided by Prof. Yong-Bin Yan and Prof. Hai-Meng Zhou (School of Life Sciences, Tsinghua University, China). Site-directed mutagenesis was performed with the QuikChange Site-Directed Mutagenesis Kit (Invitrogen, Carlsbad CA) to generate a K369Q AcetylK mimic and a S372E phospho-mimic using the primers 5'GAGAAGAAGTTGGAGCAAGGCCAGTCCA TCG and 5' GAAGTTGGAGAAAGGCCAGGAAATCGACG ACATGATCCCCG, respectively. Cells were transfected for 24 h and harvested after an additional 24 h.

Myocardial peptide preparation. Myocardial tissue was ground under liquid nitrogen and 100 mg of powdered tissue from each group pooled (i.e n=3, total 300 mg). Samples were homogenized in 3-fold the weight (i.e. 1 mg / 3 μL) of lysis buffer (20 mM Tris, 1 mM dithiothreitol (DTT), 0.5% SDS, Protease Inhibitor Cocktail (Roche, Basel, Switzerland), Phosphatase Inhibitor Cocktail III (Calbiochem, Darmstadt, Germany), 10 μM trichostatin A, 10 mM nicotinamide, 50 mM butyric acid, pH 7.5) at 4°C using an Omni homogenizer (Omni International, Kennesaw GA) followed by tip-probe sonication. The homogenate was centrifuged at 12,000 x *g* for 15 min at 4°C and the supernatant precipitated with chloroform / methanol. Proteins were resuspended in 6M urea, 2M thiourea, 50mM triethylammonium biocarbonate (TEAB), pH 8.0 and reduced with 10mM DTT for 1 h at 25°C followed by alkylation with 25mM iodoacetamide (IAA) for 30 min at 25°C in the dark. The reaction was diluted 1:10 with 50 mM TEAB and digested with trypsin (Promega, Madison WI; 50:1 substrate:enzyme) for 12 h at 30°C, acidified to 2% (v/v) formic acid

(FA), centrifuged at 12,000 x *g* for 15 min, and the supernatant removed. Peptides were desalted with hydrophilic-lipophilic balance solid phase extraction (HLB-SPE) columns (Waters Corp., Milford MA), eluted with 80% acetonitrile (ACN), 0.1% trifluoroacetic acid (TFA) and dried by vacuum centrifugation. The entire procedure was performed in duplicate.

Stable isotope labeling with tandem mass tags (TMT) and peptide enrichment. 200 µg peptide from each group was labeled with TMT (Thermo Scientific, San Jose CA) according to the manufacturer's instructions. The first replicate was labelled as follows: TMT^6-126: 0 min ischemia; TMT^6-127: 0 min ischemia with 10µM splitomicin; TMT^6-128: 20 min ischemia; TMT^6-129: 20 min ischemia with 10µM splitomicin; TMT^6-130: IPC; TMT^6-131: IPC with 10µM splitomcin. The second replicate was labelled in reverse. Peptides were resuspended in 50mM MOPS, 10mM NaH_2PO_4, 50mM NaCl (immunoprecipitation [IP] buffer; pH 7.2), supplemented with 50µL anti-AcetylK antibody conjugated agarose (ImmuneChem Pharmaceuticals, Canada), and rotated at 4°C for 16 h. The suspension was centrifuged at 1000 x *g* for 1 min and the supernatant collected. The resin was washed with 4 x 1 mL IP buffer followed by 2 x 1 mL H_2O. Lysine acetylated peptides were eluted with 2 x 200 µL 0.2% (v/v) TFA and purified using a C18 / POROS Oligo R2 / R3 reversed phase (RP) micro-column, dried by vacuum centrifugation, and stored at -20°C. The supernatants from the IP flow-through and each wash were combined, and diluted 10-fold in 1M glycolic acid in 80% ACN, 5% TFA (TiO_2 loading buffer), as described (65). This solution was incubated with 3 mg TiO_2 beads for 15 min at room temperature with gentle agitation. The suspension was then centrifuged at 1000 x *g* for 1 min. Supernatant was removed and beads washed with TiO_2 loading buffer followed by 80% ACN, 2% TFA and finally 20% ACN, 0.2% TFA. Phosphopeptides were eluted with 1% ammonium hydroxide, pH 11.3 and purified using a C18 / POROS Oligo R3 RP micro-column, dried by vacuum centrifugation and stored at -20°C. Enriched peptides were fractionated into 10 fractions for phosphopeptides and 6 fractions for AcetylK peptides respectively, using TSKGel Amide-80 HILIC capillary HPLC. (66).

Reversed phase nano liquid chromatography - electrospray ionization tandem mass spectrometry (nRPLC-ESI-MS/MS). Fractionated TMT labelled peptides were resuspended in 0.1% FA and separated by RP chromatography on an in-house 25 cm x 75 µm Reprosil-Pur C18-AQ column (3 µm; Dr. Maisch, Germany) using an EASY nLC nanoHPLC (Proxeon, Odense, Denmark). The HPLC gradient was 0-40% solvent B (A, 0.1% FA; B, 95% ACN, 0.1% FA) over 120 min at a flow of 250 nL/min. MS was performed using an LTQ-Orbitrap Velos (Thermo Scientific). An MS scan (400-2000 *m/z*; MS AGC 1 x 10^6) was recorded in the Orbitrap set at a resolution of 30,000 at 400 *m/z* followed by data dependent higher energy collision dissociation (HCD) MS/MS analysis of the 7 most intense precursor ions. Parameters for HCD were: activation time 0.1 ms, normalized energy 45 (48 for phosphopeptides), dynamic exclusion enabled with repeat count 1, resolution 7,500, exclusion duration 30 sec, maximum injection time 500 ms and MS^n AGC 1 x 10^5. Collected data are shown in Table S1.

SILAC labelled rat L6 myoblast peptides were resuspended in 0.5% acetic acid and separated by RP chromatography on an in-house 40 cm x 75 µm Reprosil-Pur C18-AQ column (1.9 µm; Dr. Maisch) using an EASY nLC-1000 nanoUHPLC (Proxeon). The HPLC gradient was 0-40% solvent B (A, 0.5% acetic acid; B, 90% ACN, 0.5% acetic acid) over 90 min at a flow of 250 nL/min. MS was performed using a Q-Exactive (Thermo Scientific). An MS scan (300-1750 *m/z*; MS AGC 3 x 10^6) was recorded in the Orbitrap set at a resolution of 70,000 at 200 *m/z* followed by data-dependent HCD MS/MS of the 12 most intense precursor ions. Parameters for HCD were: normalized energy 25, dynamic exclusion enabled, resolution 35,000, exclusion duration 60 sec, maximum injection time 120 ms and MS^n AGC 1 x 10^6.

Metabolite quantification by ion pairing LC-SRM. Metabolites were extracted from 50mg tissue using a modified boiling water extraction (67). Tissue was added to 150 µL 1 mM EDTA, 1 mM HEPES, pH 7.2, 4°C and vortexed for 20 sec. The extract was boiled for 90 sec, snap frozen in

liquid nitrogen, incubated at 25°C for 5 min and then snap frozen for 1 min. A second incubation at 25°C for 5 min was followed by incubation at -20°C for 1 h. The extract was incubated at 4°C for 10 min and centrifuged at 20,000 x *g* for 15 min at 4°C. Aliquots of 10µL supernatant were analyzed in triplicate. Metabolites were separated by RP chromatography on an in-house 320 µm x 15 cm C18-AQ (3 µm; Dr. Maisch) column. The HPLC gradient was 0-20% solvent B over 5 min, 20% for 15 min, 20-35% over 2.5 min, 35% for 2.5 min, 35-60% over 2.5 min, 60-95% over 2.5 min, 95% for 7.5 min (A, 10 mM tributylamine adjusted to pH 4.9 with 15 mM acetic acid; B, methanol) at 6 µL/min. MS was performed using a 5500 QTRAP with TurboIon spray source in negative ion MRM mode. Parameters were: GS1 20 p.s.i., curtain gas 20, ionspray voltage = -4500 V, unit-resolution. Acquisition was performed by unscheduled-MRM with a dwell time for each transition set to 100 msec. Synthetic metabolites (Sigma-Aldrich) were prepared in 10mM stock solutions. Each metabolite was directly infused into the mass spectrometer to select and optimize transitions and to determine retention times. A 10µM standard mixture was used for quality control and standard curves. LLOQ and ULOQ were assessed using a standard curve at 10 concentrations from 100pM to 10µM defined as R^2 >0.95 and coefficient of variation (CV) <20%. Standard additions experiments were performed to validate metabolite identification based on retention times but no standard addition curves were performed and therefore relative quantification is presented (Tables S2 and S3). All data analysis was performed in MultiQuant v2.0 (AB Sciex).

Assessment of splitomicin stability by LC-SRM. To ensure stability, splitomicin solutions were analysed on a 1 x 50 mm Luna Phenyl-Hexyl column (5µm; Phenomenex, Torrance, CA). The HPLC gradient was 0-100% solvent B over 5 min and 100% for 5 min (A, 0.1% acetic acid; B, acetonitrile) at 100µL/min. MS was performed using a 5500 QTRAP in positive ion MRM mode. Parameters were: GS1 20 p.s.i., GS2 25 p.s.i., curtain gas 20, ionspray voltage = 5000 V, unit-resolution. Acquisition was performed by unscheduled-MRM with a dwell time for each transition set to 100 ms. Splitomicin (Sigma-Aldrich) was prepared in a primary stock solution of 10 mM in methanol. A 10 µM solution was prepared in 50% methanol, 0.1% acetic acid and used to select and optimize transitions. A 10 µM stock solution was prepared in Buffer A and LLOQ and ULOQ assessed using a standard curve at five concentrations from 1nM to 10µM defined as R^2 > 0.95 (Figure S2A). Next, 10 µM splitomicin in phosphate-buffered saline (pH 7.5) was incubated at 37°C. At the specified times (0, 10, 20, 30, 40 min), 10 µL was removed and diluted 10-fold with Buffer A and 10 µL immediately analysed in triplicate (Figure S2B). Data analysis was performed in MultiQuant v2.0 and manually verified for peak quality (Figure S2C). Following 20 min incubation (the specified baseline period for splitomicin in heart perfusions prior to ischemia), the splitomicin concentration was reduced from 10 to 5µM, which is >10-fold the minimum inhibitory concentration (MIC) (68). At 40 min (the total time of the longest Langendorff experiment, including ischemia), the concentration still remained above the MIC.

Western blotting. 20 µg proteins were separated on 7 cm SDS-PAGE gels followed by wet transfer to PVDF membranes. All blots were blocked with 5% bovine serum albumin in Tris-buffered saline, 0.1% Tween-20 overnight at 4°C. Primary antibodies were obtained from Cell Signaling Technology (Danvers MA) and were as follows: Anti-phospho-AMPKα (T172), anti-AMPKα, anti-phospho-acetyl-CoA carboxylase (S79), anti-phospho-Akt (S473), anti-Akt, anti-phospho-eIF4B (S422), anti-eIF4B, anti-phospho-PKA substrate (RRXpS/pT). Secondary antibody was anti-rabbit IgG-HRP. Equal protein loading was confirmed with Coomassie staining.

Analysis of untargeted mass spectrometry data. Raw data were processed using Proteome Discoverer v1.3beta (Thermo Scientific) into .mgf files. TMT labelled myocardial peptides were searched against the UniProt *Rattus norvegicus* database (March 2012: 41,696 entries) using MASCOT (v1.12). SILAC labelled L6 myoblast peptides were searched against the UniProt *Rattus norvegicus* database containing an additional CKM entry containing a K369Q mutation, using SEQUEST. Searches were performed with the following fixed parameters: precursor mass tolerance of 10 ppm, product ion tolerance of 0.02 Da, Cys-carboxyamidomethylation (TMT

peptides), and 1 missed cleavage (3 for AcetylK enrichments). For TMT peptides, searches were conducted with variable modifications: oxidation of Met, TMT labeling of *N*-termini and Lys, phosphorylation of Ser, Thr, Tyr and acetylation of Lys. For SILAC peptides, variable modifications were: oxidatation of Met, SILAC labeling of Arg and Lys, phosphorylation of Ser, Thr, Tyr. Quantification was performed using Proteome Discoverer with HCD MS/MS reporter ion integration within a 50ppm window for TMT labelling and, mass prescision set to 2 ppm for SILAC labelling extracted ion chromatograms. All searches were filtered to a <1% false discovery rate (FDR) using Percolator (69). PhosphoRS probabilities were used to calculate phosphorylation site localizations and a confident site reported as >75% localization probability (70). Phosphopeptide and AcetylK peptide ratios were normalized by the median ratios of non-modified peptides in each replicate. The global effect of ischemia, IPC and splitomicin on phosphorylation and AcetylK was assessed by calculating the median of the duplicate averaged ratios. The intensity of the observed reporter ions is known to influence quantification accuracy (71). To account for this, the standard deviation of the Log_2ratios were calculated by ranking the peptide intensities and a sliding window script in R-project using the Ringo Package enabled the calculation of a peptide intensity-dependent standard deviation (72). P-values were calculated using a two-sided t-test and adjusted for multiple testing using a FDR approach (73) with the Stats Package in R-project. Peptides were considered to be significantly regulated if their ratios were >2 standard deviations (i.e *p*-value <0.05 following FDR correction) and with a cut-off of +/- 1.5-fold change within each replicate. A less stringent analysis was also utilized to investigate regulated sites with only a cut-off +/- 1.5 fold change. Fuzzy c-means cluster analysis was performed using GProX (74). Kinase-substrate predictions were made using ScanSite (75) and pathway analysis performed with Ingenuity Pathway Analysis (www.ingenuity.com).

Peptide synthesis. Peptide synthesis was performed by Fmoc chemistry (76). Briefly, peptides were prepared on a 0.25 mmole scale by manual stepwise solid-phase synthesis using benzotriazol-1-yl-1,1,3,3-tetramethyluronium / N,N-diisopropylethylamine (HBTU / DIPEA) on Rink Amide MBHA resin (substitution 0.78 mmol /g) (Novachem, Collingwood, Australia). Amino acid (5 equiv.) and DIPEA (10 equiv.) were employed in each coupling step for 10 min except for the synthesis of phosphorylated peptides, where the coupling of Fmoc-Ser[PO(OBzl)-OH]-OH was performed in 2.5 equiv. in the presence of 2-(7-aza-benzotriazole-1-yl)-1,1,3,3-tetramethyluronium hexafluorophosphate (HATU). Fmoc deprotections were achieved with 3 x 3 min in an excess of 20% piperidine in dimethylformamide (DMF), and capping achieved with 8% acetic anhydride in DMF for 10 min. Synthesis of lysine acetylated peptides was achieved with Fmoc-Lys(Mtt)-OH, which was deprotected after the final assembly with 5 x 3 min in an excess of 2.5% TFA, 2.5% triisopropylsilane (TIPS) in chloroform followed by 3 x 3 min in an excess of 10% DIPEA. Acetylation was performed with 2 x 10 min in an excess of 8% acetic anhydride in DMF. The peptides were simultaneously deprotected and cleaved from the resin in 2.5% TIPS, 2.5% H_2O in 95% TFA for 2 h. The solution was filtered and the filtrate dried under nitrogen. Peptides were precipitated with diethyl ether, resuspended in 50% ACN, lyophilized, resuspended in 0.1% TFA and purified by HPLC on a 25 cm x 15.2 mm C18 column (10 µm; Phenomenex, Torrance CA) using a GBC LC 1150 (Braeside, Australia). The HPLC gradient was 0-100% solvent B (A, 0.1% TFA; B, 90% ACN, 0.1% TFA) over 60 min at a flow of 3 mL/min with 1.5 mL fractions collected and UV detection at 210 nm. The non-acetylated peptides were purified to > 99% (according to UV), while acetylated peptides contained a minor (~9%) amount of the non-acetylated form.

***In vitro* kinase / phosphatase / acetyltransferase / deacetylase assays by nLC-SRM.** Hearts were equilibrated for 15 min with normoxic perfusion and then subjected to 20 min ischemia using Langendorff perfusion as described above. Tissue (500-600mg) was homogenized in 3-fold the weight (i.e 1mg / 3µL) of lysis buffer containing 20mM Tris, 7.5mM $MgCl_2$, protease inhibitor cocktail, pH 7.4 at 4°C. For kinase assays, lysis buffer was supplemented with 5mM ATP, phosphatase inhibitor cocktail III, and 10µM Trichostatin A, 10mM nicotinamide, and 50mM

butyric acid. For acetyltransferase assays, lysis buffer was supplemented with 1mM acetyl-CoA containing phosphatase and deacetylase inhibitor cocktails. For phosphatase / deacetylase assays, lysis buffer was supplemented with 1mM NAD. Lysates were adjusted to pH 7.4, kept at 4°C and assays performed within 30 min. Assays were performed as described for kinase activity assay for kinome profiling (KAYAK) with minor modifications (77-78). Briefly, reactions were performed with 100µg lysate and 250pmol of substrate in a final reaction volume of 20µL. Reactions were performed at 28°C and quenched with 20µL 20% trichloroacetic acid (TCA) to precipitate the lysate following 0, 10, 20, 30 and 60 min. The reactions were centrifuged at 16,000 x *g* for 15 min at 4°C, supernatants removed and diluted 1:1 with 0.2% TFA, and desalted with C18/R2/R3 micro-columns. Peptides were resuspended in 100 µL of 0.1% FA and 5 µL analyzed by nLC-SRM. Peptides were trapped on a 0.5 cm x 300 µm Zorbax C18 column (5 µm; Agilent Technologies, Palo Alto, CA) at 5 µL/min for 5 min using a nanoLC 2Dplus system (Eksigent, Dublin CA). Peptides were separated by RP chromatography on an in-house 30 cm x 75 µm Reprosil-Pur C18-AQ (3 µm; Dr. Maisch) PicoFrit column (New Objective, Woburn MA). The HPLC gradient was 0-40% solvent B (A, 0.1% FA; B, 90% ACN, 0.1% FA) over 10 min at a flow of 250 nL/min. MS was performed using a 5500 QTRAP operated in MRM mode. Parameters were: GS1 20 psi, curtain gas 20 psi, interface temperature 150°C, ionspray voltage 2200 V, unit-resolution. All 4 peptides were monitored (unscheduled) for each reaction and areas under the curve obtained using Skyline (79) and expressed as % substrate conversion [$Area_{product}/(Area_{substrate} + Area_{product})$]. Transitions were Savitzky Golay transformed and integration boundaries manually verified. All reactions were analyzed in triplicate and those with CV >20% removed. Controls were performed without addition of lysate, and incubation of the substrates at 28°C for 60 min. No significant differences in substrate peak areas were observed. Five transitions / peptide were utilized (80) (Table S4). Validation of equimolar concentrations and transition selectivity were determined by creating a quality control mix of the 4 peptides (KxxS, KxxpS, AcKxxS and, AcKxxpS) and spiking 50 fmol into a background myocardial lysate followed by TCA precipitation, desalting, and analysis by nLC-SRM (Figure S3).

Immunoprecipitation of CKM WT, K369Q and S372E and in vitro kinase / phosphatase and deacetylase assays. L6 myoblast cells were lysed in NP40 lysis buffer (25mM Tris, 137mM NaCl, 10% glycerol, 1% NP40, protease inhibitor cocktail, phosphatase inhibitor cocktail, pH 7.4) and added to protein G beads pre-incubated with anti-FLAG M2 antibody (Sigma-Aldrich). Following incubation at 4°C for 2 hr, beads were washed 3 times with NP40 lysis buffer, 3 times with PBS and once with either kinase buffer (20mM Tris, 7.5mM $MgCl_2$, 5mM ATP, 2µM $CaCl_2$, 1.2µM calmodulin, pH 7.4) or deacetylase buffer (20mM Tris, 4mM $MgCl_2$, 50µM NAD, pH 7.4). For phosphatase assays, CKM was firstly phosphorylated by resuspending the beads in 20 µL of kinase buffer containing 80U of CaMKII (New England Biolabs, MA) and reacted for 60 min at 30°C. The beads were washed 3 times with PBS and once with phosphatase buffer (20 mM Tris, 10 mM $MnCl_2$, pH 7,4) and heavy labelled samples treated with 5U of protein phosphatase 1 (PP1; New England Biolabs) for 30 or 60 min at 30°C. For deacetylase assays, the heavy labelled samples were resuspended in 20 µL of deacetylase buffer containing active FLAG-tagged SIRT1 (generously provided by Dr. Amanda Brandon, Diabetes and Obesity Program, Garvan Institute of Medical Research) and reacted for 30 or 60 min at 30°C. Elution was performed with 8 µg /30 µL of FLAG peptide in PBS, and light and heavy samples pooled. Proteins were separated by SDS-PAGE and stained with SYPRO Ruby (Invitrogen) (Figure S4) followed by in-gel tryptic digestion. The experiment was performed in two biological replicates.

Peptide analysis by Nuclear Magnetic Resonance (NMR) spectroscopy and circular dichroism (CD). Peptides were dissolved in 20 mM Tris-d_{11} (1 mM, 600 µL H_2O/D_2O 9:1) and adjusted to pH 7.2. 1D ^{1}H-NMR spectra were acquired on a Bruker Avance III 600 spectrometer (Bruker Corp., Billerica MA) with water suppression (DIPSI) at 276 – 298 K. 2D ^{1}H-NMR spectra were acquired on a Bruker Avance III 800 spectrometer with water suppression (DIPSI) at 276 K with a mixing time of 100 ms. ^{1}H chemical shifts were referenced to 4,4-dimethyl-4-silapentane-1-

sulfonic acid (DSS) (δ 0.00 ppm) in water. Spectra were processed using Topspin (Bruker) and manually analyzed with Sparky v3.114. For CD analysis, peptides were dissolved in 20 mM Tris (100 μM, 300 μL) and adjusted to pH 7.2. Analysis was performed in a 1 mm quartz cell using a Jasco (Easton, MD) spectropolarimeter (λ 185-260 nm) at 50 nm / min with a bandwidth of 1.0 nm. Each spectrum represented an average of 5 scans.

Data Availablility. MS data have been deposited into the PeptideAtlas repository (Identifier(s): PASS00283 for global quantification of phosphorylation and AcetylK following ischemia and IPC; ftp://PASS00283:RD6524nx@ftp.peptideatlas.org/ ; PASS00280 for quanification of phosphorylation and AcetylK crosstalk on CKM synthetic peptides ftp://PASS00280:LP4689mh@ftp.peptideatlas.org/ and; PASS00286 for quantification of dephosphorylation rates of S372 on human CKM with and without AcetylK ftp://PASS00286:GJ9542qa@ftp.peptideatlas.org/)

Results

Myocardial phosphorylation and AcetylK networks. To gain insights into signalling networks initiated by ischemia and IPC, we quantified protein phosphorylation and AcetylK using isobaric labelling and MS/MS. Rat hearts (n=3 per group) were isolated using an *ex vivo* Langendorff model and subjected to: i) 0 min ischemia (0I); ii) 20 min ischemia (20I); and iii) an IPC protocol (3 x 2 min I/R); all in the presence or absence of 10μM splitomicin (22) (Figure 1A). Lysates were trypsin digested and peptides labelled with TMT. Phospho- and lysine acetylated peptides were enriched by TiO_2 chromatography and immunoprecipitation, respectively; and fractionated by HILIC. These fractions were analysed by nanoLC-MS/MS and the entire procedure repeated with reverse labelling. Overall, 3,101 protein groups were modified (Table S1). Phosphorylation and AcetylK modified 2,546 and 728 protein groups, respectively, while 331 were modified by both PTMs. Quantification at the protein level was obtained for 694 protein groups (>1 peptide), with 298 and 361 of these containing either phosphorylation or AcetylK sites, respectively (Table S1). Protein abundance displayed very low variation (global Log_2 standard deviations measured at 0.31 and 0.34 for 20I and IPC, repectively), while larger variations were observed for phosphopeptides (Log_2 standard deviations of 0.58 and 0.64 for 20I and IPC) and lysine acetylated peptides (Log_2 standard deviations of 0.48 and 0.59 for 20I and IPC), suggesting the myocardial response to acute ischemia and IPC is dominated by changes in PTMs rather than protein abundance (Figure 1B). Perfusion of rat hearts with 10μM splitomicin, without subsequent ischemia or IPC, increased global AcetylK by ~10% (median ratio for 0I + splitomicin : 0I = 1.1) and phosphorylation by ~2.5%. 20I increased global phosphorylation (median ratio for 20I : 0I = 1.04) and AcetylK (median ratio = 1.05), and both were further increased by splitomicin (median ratios compared to 0I of 1.08 for phosphorylation and AcetylK, respectively). IPC decreased global AcetylK by ~10% (median ratio for IPC : 0I = 0.91), and phosphorylation by ~20% (median ratio for IPC : 0I = 0.83). Splitomicin inhibited the reduction in AcetylK (median ratio for IPC + splitomicin : 0I = 0.98), but not phosphorylation (median ratio for IPC + splitomicin : 0I = 0.81). For all conditions, total protein abundance showed median ratios that indicated a <1% change. These data suggest that ischemia and IPC influence global AcetylK and phosphorylation, and also show that modulation of AcetylK with splitomicin can influence phosphorylation indicative of crosstalk.

We quantified 7,437 unique phosphopeptides (5,605 phosphosites with >75% localization probability; Table S1), 346 (271 phosphosites; Table S1) showing >1.5-fold up-regulation and 194 (154 phosphosites) showing >1.5-fold down-regulation following 20I. Of the regulated phosphosites, 69 were significant with *p*-value <0.05 in two independent experiments and 272 with *p*-value <0.05 in at least one experiment (two-sided t-test). 402 unique phosphopeptides were regulated (299 phosphosites; Table S1) by >+/-1.5-fold following IPC (54 phosphosites with *p*-value <0.05 in two independent experiments and 197 with *p*-value <0.05 in at least one experiment). Surprisingly, 267 of these phosphopeptides were not regulated in 20I and were highlighted as IPC-specific. 2,898 unique lysine acetylated peptides were quantified, with 229 of these up- or down-

regulated (>+/-1.5-fold) following either 20I (80 peptides) or IPC (159 peptides), which was consistent with the median ratios for these conditions (Figure 1B; Table S1).

The large-scale data were interrogated using Ingenuity Pathway Analysis (IPA) to identify pathways enriched in proteins containing peptides modified by phosphorylation, AcetylK or both (Figure S5). Site-specific analysis also allowed us to highlight PTM sites differentially regulated between ischemia and IPC, and those influenced by splitomicin to determine potential targets of crosstalk. Several pathways were over-represented with regulated phospho- and AcetylK sites in both ischemia and IPC (Figure S5), including those associated with metabolism (fatty acid metabolism, TCA cycle, glycolysis; Figure 2A), as well as those involved in contraction and mitochondrial function (Figure S6). Fatty acid metabolism was enriched in both regulated phosphorylation and AcetylK sites (Figure 2A) during ischemia and IPC. Several AcetylK sites showed differential modification when compared between 20I and IPC, for example K214 of 3-ketoacyl-CoA thiolase (ACAA2) was significantly deacetylated (>1.5-fold down-regulated; *p*-value <0.05) but only during IPC. Similar data were observed for mitochondrial trifunctional enzyme subunits alpha and beta (HADHA and HADHB), which also display 3-ketoacyl-CoA thiolase activity. Splitomicin attenuated deacetylation of ACAA2 K214 (*p*-value <0.05), and additional sites on HADHA. Deacetylation events were observed more frequently in IPC than ischemia, however this effect was not global and we observed increased AcetylK on a number of sites, including additional sites on ACAA2 and HADHB, suggesting multiple acetylases / deacetylases are active during IPC. Our results also show extensive modification of proteins associated with mitochondrial dysfunction (Figure S6), including several involved in redox homeostasis and oxidative phosphorylation. IPC-specific deacetylation was observed on more than 10 subunits of complex I, however none of these sites was attenuated by splitomicin. Complex V was extensively modified with both phosphorylation and AcetylK. For example, increased acetylation of K73 on mitochondrial ATP synthase subunit O (ATP5O) was observed with splitomicin treatment following both 20I and IPC. Additional pathways included the mitochondrial permeability transition pore (mPTP) complex and the contractile apparatus (Figure S6). Tropomyosin (TPM1) in particular, contained numerous AcetylK and phosphorylation sites that were either significantly deacetylated or dephosphorylated during IPC, with this effect significantly reversed by splitomicin, which suggests co-regulation between these PTM.

Since splitomicin attenuates IPC (22) and our data identified pathways influenced by splitomicin in ischemia and IPC, we wished to validate the functional basis for these changes. The production and utilization of high-energy phosphates are metabolic processes intimately associated with ischemia and IPC. These pathways (e.g. TCA cycle, glycolysis) were over-represented as containing PTM sites responding to ischemia and / or IPC (Figure 2A; Figure S5). We attempted to validate our PTM data and pathway analysis using metabolomics assays quantified by LC selected reaction monitoring (LC-SRM) (Table S2). We monitored succinyl-CoA (TCA cycle), fructose-1,6-bisphosphate (glycolysis) and creatine phosphate (mitochondrial high-energy phosphate essential for muscle contraction), as well as co-factors (NAD, NADH and NADP) and lactate (Figure 2B). Fructose-1,6-bisphosphate levels remained unaltered compared with 0I in both 20I and IPC, irrespective of splitomicin treatment. Succinyl-CoA however, increased >5-fold following 20I and this was attenuated by splitomicin. Several AcetylK sites were identified on succinyl-CoA ligase (SUCLA2; Figure 2A), yet only K88 was deacetylated during ischemia and ameliorated to control levels by splitomicin in a manner consistent with the metabolite data. No alterations in succinyl-CoA levels were observed in IPC. Creatine phosphate was reduced by >40-fold after 20I, irrespective of splitomicin treatment, however splitomicin in IPC resulted in creatine phosphate levels significantly higher than those observed in IPC alone. We identified AcetylK sites in both muscle-type creatine kinase (CKM) and creatine kinase mitochondrial-type 2 (CKMT2) that were regulated by ischemia and IPC, and a subset of these responded to splitomicin (Figure S6). Ischemia induced accumulation of NADH, yet NAD^+ and NADP were unaltered relative to 0I. As expected, lactate increased by >40-fold after 20I,

however splitomicin attenuated this significantly. Our data suggest this is unrelated to lactate oxidation, since splitomicin did not influence NADH levels.

AcetylK influences kinase activation during myocardial ischemia and IPC. Crosstalk between phosphorylation and AcetylK is likely mediated by kinases / phosphatases and / or acetylases / deacetylases. To test this, we employed splitomicin inhibition of lysine deacetylation, and examined alterations in signal pathways and their kinases. Firstly, phosphopeptides up-regulated by >1.5-fold in 20I were clustered into 2 groups: i) those unaltered, and ii) those responding, to splitomicin (Figure 3A,B). These clusters were subjected to IPA analysis (Figure S5B,C). Enriched pathways containing proteins showing phosphorylation increases in 20I that were ameliorated by splitomicin (Figure 3B; Figure S5C) included AMPK signalling, insulin receptor signalling (taken as AKT) and PKA signalling, while those that did not respond to splitomicin were predominantly associated with metabolism (glycolysis / gluconeogenesis), aldosterone and actin signalling, ubiquitination and extracellular remodelling (Figure S5B). Site-specific analysis was performed on phosphopeptides regulated during 20I that responded to splitomicin, and a subset of these mapped onto a network centred on AMPK, PKA and AKT (Figure 3C). Many substrates of these kinases were regulated by 20I and the phosphorylation changes ameliorated by splitomicin. This shows a role for AcetylK in regulating AMPK and AKT during myocardial ischemia, and is the first report to suggest a role for AcetylK in PKA regulation.

Western blotting confirmed the effects of splitomicin on phosphorylation of AMPK, AKT, PKA and their substrates (Figure 3D,E; Figure S7). For these experiments, we generated hearts over a time-course of ischemia (0, 2, 10, 20 min ischemia; n=3) compared to 20 min free perfusion (or 'time control'; TC; n=3). Splitomicin attenuated ischemia-induced phosphorylation of T172 on αAMPK and S473 on AKT, and this effect was more pronounced at 20I (Figure 3D). The downstream targets of AMPK (S79 on ACC) and AKT (S422 on eukaryotic initiation factor 4B) were regulated similarly to their respective kinases (Figure 3D). S79 phosphorylation inhibits ACC activity (carboxylation of acetyl-CoA to malonyl-CoA), however splitomicin in 20I did not result in a concomitant decrease in acetyl-CoA, as determined by LC-SRM (Figure 3F; Table S3), despite the reduction in ACC phosphorylation. This suggests AcetylK / deacetylation may influence other enzymes with acetyl-CoA as a substrate or product (e.g 3-ketoacyl-CoA thiolase). Citrate and other small molecules also allosterically modulate ACC activity (81). Ischemic phosphorylation of PKA substrates (RRXpS/pT) was also attenuated by splitomicin (Figure 3E). This correlated with splitomicin attenuation of ischemia-associated increases in cAMP, and provided evidence that PKA activation may be regulated by AcetylK / deacetylation *via* modulation of cAMP levels (Figure 3G; Table S3).

We next investigated kinase activation in IPC. Phosphopeptides up-regulated by >1.5-fold were functionally clustered using IPA (Figure S5D). Enriched pathways included PKA, α-adrenergic and calcium signalling. A common feature of these is MAPK signalling. We identified increased phosphorylation of Y185 in the activation loop of MAPK1 and Y205 on MAPK3, both of which are associated with IPC (82). We did not however, observe altered phosphorylation of a variety of PKC isoforms or substrates, including PKCA / PKCB (T497 / T550) and PKCD (T505); nor the activation autophosphorylation site of PKCD (S643), the activation *C*-terminal hydrophobic site of PKCD (S662), or of PKCE (S729). Phosphopeptides up-regulated by >1.5-fold in IPC were next clustered into 2 groups: i) those unaltered, and ii) those ameliorated, by splitomicin, and each analysed using IPA (Figure S5E,F). In contrast to the results from 20I, PKA signalling was the most enriched pathway unaffected by splitomicin treatment. Enriched pathways in the cluster containing phosphopeptides ameliorated by splitomicin were predominantly associated with cell junction signalling, as well as AMPK signalling (consistent with the results observed in 20I +/- splitomicin).

AcetylK promotes dephosphorylation in a basophilic kinase motif. Our large-scale data show strong evidence for crosstalk - phosphorylation and AcetylK co-occurred on many proteins, both PTM could be influenced by splitomicin, and inhibition of lysine deacetylation influenced activation of 3

kinases (AMPK, AKT and PKA) and their downstream targets. We next examined the sequence context and structural basis of crosstalk by determining the proximity of PTM in tertiary structures (Protein Data Bank; PDB) of 45 proteins containing at least one confident ischemia or IPC regulated phosphorylation / AcetylK site. Of these, 25 structures were available in the Mammalia taxonomy containing at least 80% sequence similarity to the Swiss-Prot *Rattus norvegicus* sequence. Three proteins contained an amino acid substitution at one site of PTM observed here. Fourteen proteins contained at least one observed phosphorylated residue within ~10 Å of an identified acetylated lysine (Figure S8). For example, the solution structure of TPM1 highlights head-to-tail interactions between individual molecules where the *C*-terminal phosphorylation on S283 is in close proximity to an *N*-terminal acetylation on K12. Proximal modifications were both adjacent (<5 amino acids) and distant (>5 amino acids) in the primary sequence.

We next attempted to identify sequence motifs in which phosphorylation and AcetylK were over-represented. MS/MS sequences from PTM analysis of ischemia and IPC were combined, and those showing evidence of modification by both considered further. We identified 50 peptides containing the basophilic protein kinase motif KxxS, modified with either AcetylK or phosphoserine, but not both simultaneously (Table S5). For example, CKM was modified by AcetylK at K369 or phosphorylation at S372 and both sites were regulated by >1.5-fold following 20I. These changes were partially attenuated by splitomicin (Table S1).

To investigate this crosstalk and the rates of modification induced by proximal PTM in the KxxS motif, we synthesized the *C*-terminal peptide from CKM (^{364}EKKLEKGQSIDD^{375}) as 4 variants: i) non-modified (KxxS); ii) phosphorylated at S9 (equivalent to S372; KxxpS); iii) acetylated at K6 (K369; AcKxxS) and; iv) acetylated at K6 and phosphorylated at S9 (K369 and S372; AcKxxpS). We performed *in vitro* kinase, phosphatase, acetyltransferase and deacetylase reactions on all variants and monitored the substrates and products by nLC-SRM. Each variant was spiked into a separate lysate generated following 20I. Quantification was performed by comparing the area under the curve of the product / substrate and expressed as % substrate conversion / min. Initially, kinase reactions were performed seperately on the two non-phosphorylated substrates (+/- AcetylK) in the presence of 5 mM ATP, phosphatase and deacetylase inhibitors. Maximum phosphorylation of the KxxS substrate was observed after 20 min (13% substrate conversion of KxxS to KxxpS), however no conversion of AcKxxS to AcKxxpS was observed (Figure 4A; Table S6). Dephosphorylation was next measured for the two phosphorylated substrates (+/- AcetylK) in the presence and absence of phosphatase and deacetylase inhibitors. The KxxpS substrate displayed 4% dephosphorylation to KxxS irrespective of the presence of inhibitors, while the AcKxxpS substrate showed 70% dephosphorylation to AcKxxS within 60 min (Figure 4B; Table S6B) in the absence of phosphatase inhibition, and 33% dephosphorylation to AcKxxS in the presence of phosphatase inhibitors (Figure 4C; Table S6C). No changes in acetylation / deacetylation were observed for any of the test peptides, even in the absence of deacetylase inhibitors and in the presence of 1 mM NAD, or with added 1 mM acetyl-CoA (Tables S6D-E). These results suggest that AcetylK at the 'minus 3 amino acids' position (P-3) to the phosphorylation site promotes dephosphorylation. To further investigate this, the *C*-terminal CKM phosphopeptide was synthesized with: i) Gln at K6 (K to Q; QxxpS) to mimic AcetylK; and ii) Arg at K6 (K to R; RxxpS) to mimic the positively charged lysine. The RxxpS substrate displayed 7% dephosphorylation to RxxS, while the QxxpS AcetylK mimic showed 43% dephosphorylation to QxxS, providing further evidence for the promotion of dephosphorylation by the presence of AcetylK at P-3 (Figure 4D; Table S6F).

The hypothesis that dephosphorylation is promoted by proximal AcetylK requires the protein to be initially modified, even transiently, at both sites. To investigate this, kinase and phosphatase assays were performed using purified recombinant enzymes. ScanSite suggested that phosphorylation of CKM S372 is most likely catalyzed by calcium/calmodulin-dependant protein kinase II (CaMKII). CaMKII-mediated reactions were performed using the KxxS and AcKxxS CKM

peptides. Maximum phosphorylation of the KxxS substrate was observed after 60 min (98% substrate conversion to KxxpS), while conversion of the AcKxxS substrate proceeded at a slower rate (67% substrate conversion to AcKxxpS by 60 min) (Figure 4E; Table S6G). These results show that simultaneous phosphorylation and AcetylK can occur *in vitro*. Next, antarctic phosphatase reactions were performed on the two phosphorylated substrates (+/- AcetylK). The KxxpS substrate displayed 65% dephosphorylation to KxxS while AcKxxpS displayed a faster dephosphorylation rate (91% substrate conversion to AcKxxS within 60 min) (Figure 4F; Table S6H). Reactions were also performed on the mimic phosphopeptides, with the RxxpS substrate displaying slower dephosphorylation compared to the QxxpS AcetylK mimic (Figure 4G; Table S6I).

We next investigated AcetylK-induced dephosphorylation of full-length CKM. FLAG-tagged CKM wild-type (WT) and a K369Q AcetylK mimic were over-expressed in L6 myoblasts grown in light and heavy stable isotope labelling by amino acids in cell culture (SILAC) (Figure 5A). Following anti-FLAG immunoprecipitation, enriched WT and K369Q mimic from both light and heavy cells were subjected to *in vitro* CaMKII kinase reactions. Excess kinase was removed and the heavy labelled WT and K369Q CKM subjected to either 30 or 60 min phosphatase reactions using recombinant protein phosphatase 1 (PP1). Heavy labelled, phosphatase treated CKM was mixed with light labelled non-phosphatase treated CKM, digested with trypsin and the rate of dephosphorylation measured by nLC-MS/MS. Dephosphorylation rates were then determined by comparing the phosphopeptide heavy/light ratios. WT CKM treated with PP1 for 30 and 60 min displayed very little dephosphorylation at S372 (<1.1-fold by 60 min or phosphorylation decrease of only 3% +/- 2%; Figure 5B; Table S7). The K369Q AcetylK mimic however, displayed significant dephopshorylation of S372 by 30 min (phosphorylation decrease of 68% +/- 2%) and >2-fold dephosphorylation following 60 min (Figure 5B). These assays show that AcetylK in the KxxS kinase motif reduces the rate of phosphorylation and promotes rapid dephosphorylation.

To investigate whether phosphorylation influenced deacetylation, FLAG-tagged CKM WT and a S372E phospho-mimic were over-expressed in L6 myoblasts grown in light and heavy SILAC (Figure 5C). Following anti-FLAG immunoprecipitation, heavy labelled WT and S372E CKM were subjected to 30 and 60 min incubation with immunoprecipitated FLAG-tagged SIRT1 deacetylase. Heavy labelled, deacetylase treated CKM was mixed with light labelled non-treated CKM, digested with trypsin and deacetylation measured by nLC-MS/MS. S372E CKM treated with SIRT1 displayed only minor deacetylation at K369 (1.1-fold by 60 min, AcetylK decrease of ~10% +/- 1%; Figure 5D; Table S8). WT CKM however, displayed significant SIRT1-mediated deacetylation of K369 (1.6-fold by 60 min, AcetylK decrease of 38% +/- 3%; Figure 5D). These data suggest that phosphorylation inhibits SIRT1-mediated deacetylation within the KxxS motif. The mutually exclusive nature of these two PTMs in the large-scale *ex vivo* dataset combined with the *in vitro* assays performed here suggests that AcetylK promotes dephosphorylation, which in turn promotes deacetylation. The deacetylated form of the motif can then be phosphorylated, which is consistent with both our synthetic peptide and recombinant CKM protein kinase / phosphatase assays.

AcetylK disrupts a phosphate-lysine salt-bridge and induces peptide backbone flexibility. We next investigated the mechanism of AcetylK-induced dephosphorylation. To examine whether peptide backbone conformational changes were induced by AcetylK and / or phosphorylation, we analyzed the 4 CKM peptide variants by ^{1}H NMR in the presence of 10% D_2O in H_2O at pH 7.2 (Figure S9). 1D ^{1}H NMR of the NH region of the 4 variants highlighted only minor chemical shift differences between KxxS and AcKxxS with one additional peak arising from the acetyl amide proton (Figure S9A,B). Phosphorylation induced larger chemical shifts, and comparison of KxxpS and AcKxxpS highlighted differences that indicated significant changes in peptide backbone environments (Figure S9C,D). We investigated these by 2D ^{1}H NMR total correlation spectroscopy (TOCSY) and Nuclear Overhauser effect spectroscopy (NOESY) (Figure S10). An

overlay of HA-HN TOCSY region of KxxpS and AcKxxpS highlighted chemical shift differences in residues K6-D12, while K3-E5 was unaltered (Figure 6A). Overlay of the HB-HN TOCSY and NOESY region of AcKxxpS highlighted additional peaks in the TOCSY spectrum from residues I10-D12 that are absent in the NOESY region, indicating that the *C*-terminal region may be in two conformations (Figure 6B). These peaks were absent for KxxpS, indicating a more rigid conformation. Multiple long-range ^{1}H-^{1}H NOEs between the K6 and pS9 side chains in KxxpS, which were absent in AcKxxpS, indicated that these two residues are in close proximity (Figure 6C) and provide evidence for a phosphate – lysine interaction, which is inhibited by AcetylK. The rigidity of the KxxpS variant prompted us to investigate the presence of secondary structure. Interrogation of the NOESY spectrum revealed no HA-HN or HA-HB ^{1}H-^{1}H NOEs between *i* and *i* + 2 or 3 amino acids (indicative of α-helices). This was further confirmed by analysis of the 4 variants with circular dichroism (CD) spectroscopy, which revealed no obvious secondary structure (Table S9). Taken together, these results suggest that the KxxpS variant is in a fixed conformation due to the formation of a phosphate-lysine salt-bridge (Figure 6D). AcetylK inhibits the salt-bridge and results in a more flexible conformation, which is more accessible to phosphatases.

Discussion

Large-scale AcetylK and phosphorylation analysis in myocardial ischemia and IPC identified PTM sites not previously associated with injury or cardioprotection, and confirmed that a specific response to each occurs at the signal level. Ischemia induces extensive metabolic changes and AcetylK is emerging as a regulator of metabolism (58,63), cell protection and signal propagation (35,38). Splitomicin treatment confirmed AcetylK is involved in myocardial ischemia and IPC, and is capable of crosstalk with phosphorylation-mediated signaling. We confirmed that AcetylK influences AMPK and AKT activation, and also revealed a role in PKA regulation, most likely *via* cAMP levels, although it remains unclear whether this occurs through alteration of adenylate cyclase activity. Ischemia-induced phosphorylation of PKA site S16 on phospholamban (PLN) was attenuated with splitomicin. Phospho-S16 increases Ca^{2+} uptake into the sarcoplasmic reticlulum (SR) by disrupting the inhibitory PLN:SR-Ca^{2+}-ATPase complex (83-84). In contrast, dephosphorylation of PLN S16 / S17 was observed in IPC, and was unaffected by splitomicin, along with other PKA targets, suggesting that the loss of cardioprotection associated with splitomicin is independent of PKA. Numerous other targets of PKA were identified in the ischemia cluster responding to splitomicin (e.g. S156 on Bcl2 antagonist of cell death (BAD)), however not all PKA targets responded similarly, for example cardiac myosin binding protein C (MYBPC3) and cardiac troponin I (TNNI3) did not display increased phosphorylation in 20I nor reduced phosphorylation post-splitomicin treatment. PKA phosphorylation of S434 on SIRT1 increases deacetylase activity independently of NAD^{+} (39), suggesting SIRT1 and PKA may regulate each other in a similar fashion to SIRT1 and AMPK (17), although unlike SIRT1/AMPK, the SIRT/PKA relationship appears to be specific to ischemia. Although our study used splitomicin to inhibit lysine deacetylation (22,85), we cannot unequivocally state that AcetylK sites altered by splitomicin are direct targets of SIRT1, nor whether other SIRTs (or non-SIRT acetylases / deacetylases) may be affected. For example, members of metabolic pathways containing ischemia or IPC-induced changes in AcetylK may also be targets of SIRT3 (86). A detailed investigation of the IC_{50} values of splitomicin on other deacetylases has not been performed. Therefore, further validation of the regulated targets is required to unequivocally pinpoint the role of SIRT1.

Phosphoproteomics showed no direct evidence for PKC activation during IPC. Despite this, we did observe increased phosphorylation of MAPK variants, consistent with the model of IPC proposed in (82), which shows MAPK activation in IPC is PKC-dependent. Alternatively, our model did not examine I/R post-IPC. The PKC-epsilon isoform implicated in signal complex formation and IPC-mediated signaling (87) may be only transiently activated during one of the cycles of I/R that constitute IPC, or indeed may be downstream of alternative signal pathways implicated in IPC or I/R, for example PKC activation itself may be downstream of the ERK- and PI3K/AKT-

associated reperfusion injury salvage kinase (RISK) pathway (88) and thus may occur upon I/R after the protective IPC period is concluded.

Among the functional clusters containing members with ischemia- and / or IPC-associated peptides that were influenced by splitomicin were the contractile apparatus and mPTP. Regulation of contractility *via* phosphorylation has been demonstrated on many proteins including cardiac MYBPC3, TPM1, troponins TnI and TnT, and myosin light chains 1 and 2. Our study suggests AcetylK may play a similar role in regulating the contractile apparatus. For example, 28 AcetylK sites were identified on TPM1 and the proximity of AcetylK and phosphorylation in head-to-tail structures of TPM1 suggested PTM crosstalk is possible. Permeabilization and / or rupture of the mitochondrial membrane are linked to apoptotic and necrotic cell death, which are associated with the mPTP in ischemic injury. The molecular composition of the mPTP is still not fully unraveled, however proposed members include hexokinase 2, ADP/ATP translocase (SLC25A), VDAC, CKMT2, mitochondrial apoptosis-induced channel, and peptidylprolyl isomerase (89-91). Genetic studies however, suggest some of these may be dispensable for mitochondria-associated cell death (92-93). Recently, a novel composition of the mPTP has been proposed (94) and includes ATP synthase, which suggests a dual function for complex V; i) to produce energy and, ii) to control cell death. We identified extensive phosphorylation (>30 sites) and AcetylK (33 sites) of mPTP members, many of which were regulated by ischemia and / or IPC. Splitomicin ameliorated changes to acetylated peptides observed in ischemia and IPC from CKMT2 and SLC25A4, providing further evidence of a widespread role for lysine deacetylation in mediating the functional effects of ischemia and cardioprotection.

Another cluster of modified peptides belonged to proteins involved in fatty acid metabolism. Unlike other tissues, the myocardium produces ~60-70% of its energy from fatty acid oxidation. Ischemia results in lowered fatty acid oxidation and an accumulation of fatty acid intermediates, which have detrimental effects including increased membrane instability, arrhythmias and increased infarct size. Reducing fatty acid metabolism and promoting glucose oxidation has long been known to provide cardioprotection (95). Our data show that at least 3 enzymes (ACAA2, HADHA, HADHB) with 3-ketoacyl-CoA thiolase activity contained PTM that were induced by ischemia and / or IPC, and ACAA2 AcetylK was ameliorated in IPC by splitomicin. Inhibition of 3-ketoacyl-CoA thiolase activity with trimetazidine reduces beta-oxidation of fatty acids, promotes glucose oxidation and is a clinically effective anti-angina strategy (96). Differential regulation of AcetylK between ischemia and IPC on enzymes displaying 3-ketoacyl-CoA thiolase activity provides insight into the potential mechanism of cardioprotection.

Ischemia and IPC induced different changes to pathways involved in metabolism and the production or utilization of high-energy phosphates. Conversion to anaerobic glycolysis and production of lactate is well characterized in ischemia, and we were surprised that splitomicin ameliorated this to a significant extent. This suggests lysine deacetylation may be beneficial in ischemia, which is contradictory to the loss of cardioprotection (22) induced by splitomicin in IPC. Ischemia resulted in a similar rise in succinyl-CoA levels that were also attenuated by splitomicin. This correlated with attenuated deacetylation of at least one site in SUCLA2 suggesting a link between AcetylK and SUCLA2 activity. The large reduction in creatine phosphate seen in both ischemia and IPC was only attenuated by splitomicin during cardioprotection. These results were consistent with several PTM on both CKM and CKMT2, which again suggests that individual modification sites may be critical for activity and be influential in contributing to the ischemic or cardioprotective phenotype. Changes in the function of metabolic enzymes, such as CKMT2 and SUCLA2, which utilize the high energy ATP pool that is rapidly depleted during ischemia, may thus also be involved in maintenance of ATP levels during IPC, with their functions at least partially regulated by PTM.

Methylation in kinase motifs (97-101) and acetylation (102) can occur mutually exclusively to phosphorylation. The structural basis for crosstalk is thought to be primarily *via* steric hindrance and / or disruption of salt-bridges or hydrogen bonds between substrate and kinase (103). Contrary to this, acetylation of K105 on CDC6 results in increased phosphorylation of adjacent S106 by

cyclin-dependent kinases (CDKs) (45) and co-modification of K9 and S10 on histone H3 also occurs (104). Therefore, these PTMs can co-occur and crosstalk may mostly contribute to the kinetics of modification. A systematic investigation of neighboring modifications in the protein kinase KxxS motif was undertaken to determine the structural and kinetic constraints for crosstalk, since this motif was over-represented in PTM regulated by ischemia and IPC. Modelling of the motif using modified variants of the *C*-terminal CKM peptide (acetylation of K369 and phosphorylation of S372) showed that AcetylK induced a >10-fold dephosphorylation suggesting the recruitment of one, or more, phosphatases. This effect was also observed on full-length CKM containing a K369Q Acetyl K mimic. Although the recruitment of a phosphatase by AcetylK has been suggested (46), the molecular mechanism mediating this interaction has not previously been investigated. Our data confirmed that the KxxpS substrate contains a salt-bridge interaction between lysine and phosphate, and a peptide backbone conformational change compared to the doubly modified AcKxxpS substrate. We propose that the K-pS interaction inhibits phosphatase access while acetylation neutralizes the charge, inhibits salt-bridge formation and induces a flexible peptide backbone facilitating phosphatase access.

In vitro SIRT1 deacetylase assays of CKM WT and a S372E phospho-mimic further suggest that once dephosphorylated, the peptide is then more amenable to SIRT1-mediated deacetylation and hence may once again become available for phosphorylation, depending on the rate of protein turnover and the availability of the kinase(s) and acetylase(s) / deacetylase(s) that drive the modifications. Additionally, since the acetylase / deacetylase assays with CKM synthetic *C*-terminal peptides in complex lysates did not show a similar effect, other acetylases / deacetylases (beyond SIRT1) may be involved in mainitaing the PTM balance in cardiac tissue during I/R and/or IPC.

Fifty peptides regulated in ischemia and / or IPC contained the KxxS motif. We did not however, observe evidence for 'reciprocal' regulation (i.e. increase in the acetylated form of a peptide corresponding to a decrease in the phosphorylated form or *vice versa*), nor did we see examples of any doubly modified peptides in these data. For the structural and enzymatic evidence we observed to be physiologically relevant, the doubly modified form must be able to occur *in vivo*. We proved that phosphorylation of both the CKM *C*-terminal peptide and full-length protein can occur when lysine acetylated, albeit at a much slower rate than the native forms. These data, combined with the rapid dephosphorylation of lysine acetylated synthetic peptide variants and full-length K369Q CKM, suggest any doubly modified forms within the KxxS motif would be highly transient and therefore it is not surprising that these were not observed as they are likely to be present at extremely low abundance in the complex tissue lysates used for large-scale analysis. The lack of apparent reciprocal regulation is also likely to be due to the sub-stoichiometric levels of these (and indeed most) PTMs in the context of the overall protein abundance. This means PTM crosstalk in this context is likely involved in signal 'dampening' or 'tuning' (e.g. to protect against uncontrolled signal pathway activation) rather than acting as a strict 'on' / 'off' switch for every copy of the protein, or by generating an extreme reversal of the PTM state. Crosstalk in this motif likely provides a mechanism to modulate the level of signal activation and thus ensure the maintenance of cellular balance. To our knowledge, this is the first study to perform a detailed investigation of intra-molecular crosstalk between phosphorylation and AcetylK within a kinase consensus motif. We believe that the observed mechanism represents a previously unexplored level of regulation that is potentially widespread and is likely to involve other signalling proteins and PTMs.

Acknowledgments

This work was funded by the National Health and Medical Research Council (NHMRC) of Australia (Project Grant 571002 to S.J.C. and B.D.H.), the Lundbeck Foundation (Junior Group Leader Fellowship and LTQ-Orbitrap Velos to M.R.L.) and the Danish Natural Science Research Council (09-06-5989 to M.R.L.). B.L.P. was supported by a University of Sydney Medical Alumni Postgraduate Award. N.E.S.

and M.Y.W. are recipients of Australian Research Council Discovery Early Career Researcher Awards (DECRA). We thank Lene Jakobsen, Melanie Schulz, Ann Kwan, Kiersten Liddy, Alistair Edwards, Ben Crossett, Nestor Solis and Rima Chaudhuri for useful discussions and instrument support.

References

1. Karmazyn, M., Moffat, M.P. (1993) Na+/H+ exchange and regulation of intracellular Ca2+. *Cardiovasc. Res.* **27,** 2079-2080

2. Liu, B., Clanachan, A.S., Schulz, R., Lopaschuk, G.D. (1996) Cardiac efficiency is improved after ischemia by altering both the source and fate of protons. *Circ. Res.* **79,** 940-948

3. Armstrong, S.C. (2004) Protein kinase activation and myocardial ischemia/reperfusion injury. *Cardiovasc. Res.* **61,** 427-436

4. Hausenloy, D.J., Yellon, D.M. (2006) Survival kinases in ischemic preconditioning and postconditioning. *Cardiovasc. Res.* **70,** 240-253

5. Rose, B.A., Force, T., Wang, Y. (2010) Mitogen-activated protein kinase signaling in the heart: angels versus demons in a heart-breaking tale. *Physiol. Rev.* **90,** 1507-1546

6. Barnett, M.E., Madgwick, D.K., Takemoto, D.J. (2007) Protein kinase C as a stress sensor. *Cell Signal.* **19,** 1820-1829

7. Budas, G.R., Churchill, E.N., Mochly-Rosen, D. (2007) Cardioprotective mechanisms of PKC isozyme-selective activators and inhibitors in the treatment of ischemia-reperfusion injury. *Pharmacol. Res.* **55,** 523-536

8. Palaniyandi, S.S., Sun, L., Ferreira, J.C., Mochly-Rosen, D. (2009) Protein kinase C in heart failure: a therapeutic target? *Cardiovasc. Res.* **82,** 229-239

9. Mullonkal, C.J., Toledo-Pereyra, L.H. (2007) Akt in ischemia and reperfusion. *J. Invest. Surg.* **20,** 195-203

10. Diviani, D., Dodge-Kafka, K.L., Li, J., Kapiloff, M.S. (2011) A-kinase anchoring proteins: scaffolding proteins in the heart. *Am. J. Physiol. Heart Circ. Physiol.* **301,** H1742-1753

11. Sanada, S., Asanuma, H., Tsukamoto, O., Minamino, T., Node, K., Takashima, S., Fukushima, T., Ogai, A., Shinozaki, Y., Fujita, M., Hirata, A., Okuda, H., Shimokawa, H., Tomoike, H., Hori, M., Kitakaze, M. (2004) Protein kinase A as another mediator of ischemic preconditioning independent of protein kinase C. *Circulation* **110,** 51-57

12. Dyck, J.R., Kudo, N., Barr, A.J., Davies, S.P., Hardie, D.G., Lopaschuk, G.D. (1999) Phosphorylation control of cardiac acetyl-CoA carboxylase by cAMP-dependent protein kinase and 5'-AMP activated protein kinase. *Eur. J. Biochem.* **262,** 184-190

13. Kudo, N., Barr, A.J., Barr, R.L., Desai, S., Lopaschuk, G.D. (1995) High rates of fatty acid oxidation during reperfusion of ischemic hearts are associated with a decrease in malonyl-CoA levels due to an increase in 5'-AMP-activated protein kinase inhibition of acetyl-CoA carboxylase. *J. Biol. Chem.* **270,** 17513-17520

14. Lopaschuk, G.D., Spafford, M.A., Davies, N.J., Wall, S.R. (1990) Glucose and palmitate oxidation in isolated working rat hearts reperfused after a period of transient global ischemia. *Circ. Res.* **66,** 546-553

15. Oliver, M.F., Opie, L.H. (1994) Effects of glucose and fatty acids on myocardial ischaemia and arrhythmias. *Lancet* **343,** 155-158

16. Kahn, B.B., Alquier, T., Carling, D., Hardie, D.G. (2005) AMP-activated protein kinase: ancient energy gauge provides clues to modern understanding of metabolism. *Cell Metab.* **1,** 15-25

17. Canto, C., Gerhart-Hines, Z., Feige, J.N., Lagouge, M., Noriega, L., Milne, J.C., Elliott, P.J., Puigserver, P., Auwerx, J. (2009) AMPK regulates energy expenditure by modulating NAD+ metabolism and SIRT1 activity. *Nature* **458,** 1056-1060

18. Ruderman, N.B., Xu, X.J., Nelson, L., Cacicedo, J.M., Saha, A.K., Lan, F., Ido, Y. (2010) AMPK and SIRT1: a long-standing partnership? *Am. J. Physiol. Endocrinol. Metab.* **298,** E751-760

19. Lynn, E.G., McLeod, C.J., Gordon, J.P., Bao, J., Sack, M.N. (2008) SIRT2 is a negative regulator of anoxia-reoxygenation tolerance via regulation of 14-3-3 zeta and BAD in H9c2 cells. *FEBS Lett.* **582,** 2857-2862

20. Alcendor, R.R., Gao, S., Zhai, P., Zablocki, D., Holle, E., Yu, X., Tian, B., Wagner, T., Vatner, S.F., Sadoshima, J. (2007) Sirt1 regulates aging and resistance to oxidative stress in the heart. *Circ. Res.* **100,** 1512-1521

21. Alcendor, R.R., Kirshenbaum, L.A., Imai, S., Vatner, S.F., Sadoshima, J. (2004) Silent information regulator 2alpha, a longevity factor and class III histone deacetylase, is an essential endogenous apoptosis inhibitor in cardiac myocytes. *Circ. Res.* **95,** 971-980

22. Nadtochiy, S.M., Redman, E., Rahman, I., Brookes, P.S. (2011) Lysine deacetylation in ischaemic preconditioning: the role of SIRT1. *Cardiovasc. Res.* **89,** 643-649

23. Berger, S.L. (2007) The complex language of chromatin regulation during transcription. *Nature* **447,** 407-412

24. Latham, J.A., Dent, S.Y. (2007) Cross-regulation of histone modifications. *Nat. Struct. Mol. Biol.* **14,** 1017-1024

25. Lee, J.S., Smith, E., Shilatifard, A. (2010) The language of histone crosstalk. *Cell* **142,** 682-685

26. Strahl, B.D., Allis, C.D. (2000) The language of covalent histone modifications. *Nature* **403,** 41-45

27. Cheung, P., Tanner, K.G., Cheung, W.L., Sassone-Corsi, P., Denu, J.M., Allis, C.D. (2000) Synergistic coupling of histone H3 phosphorylation and acetylation in response to epidermal growth factor stimulation. *Mol. Cell* **5,** 905-915

28. Lo, W.S., Trievel, R.C., Rojas, J.R., Duggan, L., Hsu, J.Y., Allis, C.D., Marmorstein, R., Berger, S.L. (2000) Phosphorylation of serine 10 in histone H3 is functionally linked in vitro and in vivo to Gcn5-mediated acetylation at lysine 14. *Mol. Cell* **5,** 917-926

29. Kim, J., Guermah, M., McGinty, R.K., Lee, J.S., Tang, Z., Milne, T.A., Shilatifard, A., Muir, T.W., Roeder, R.G. (2009) RAD6-Mediated transcription-coupled H2B ubiquitylation directly stimulates H3K4 methylation in human cells. *Cell* **137,** 459-471

30. Guccione, E., Bassi, C., Casadio, F., Martinato, F., Cesaroni, M., Schuchlautz, H., Luscher, B., Amati, B. (2007) Methylation of histone H3R2 by PRMT6 and H3K4 by an MLL complex are mutually exclusive. *Nature* **449,** 933-937

31. Shi, X., Hong, T., Walter, K.L., Ewalt, M., Michishita, E., Hung, T., Carney, D., Pena, P., Lan, F., Kaadige, M.R., Lacoste, N., Cayrou, C., Davrazou, F., Saha, A., Cairns, B.R., Ayer, D.E., Kutateladze, T.G., Shi, Y., Cote, J., Chua, K.F. et al (2006) ING2 PHD domain links histone H3 lysine 4 methylation to active gene repression. *Nature* **442,** 96-99

32. Wang, Z., Zang, C., Cui, K., Schones, D.E., Barski, A., Peng, W., Zhao, K. (2009) Genome-wide mapping of HATs and HDACs reveals distinct functions in active and inactive genes. *Cell* **138,** 1019-1031

33. Zippo, A., Serafini, R., Rocchigiani, M., Pennacchini, S., Krepelova, A., Oliviero, S. (2009) Histone crosstalk between H3S10ph and H4K16ac generates a histone code that mediates transcription elongation. *Cell* **138,** 1122-1136

34. Fenton, T.R., Gwalter, J., Cramer, R., Gout, I.T. (2010) S6K1 is acetylated at lysine 516 in response to growth factor stimulation. *Biochem. Biophys. Res. Commun.* **398,** 400-405

35. Lan, F., Cacicedo, J.M., Ruderman, N., Ido, Y. (2008) SIRT1 modulation of the acetylation status, cytosolic localization, and activity of LKB1. Possible role in AMP-activated protein kinase activation. *J. Biol. Chem.* **283,** 27628-27635

36. Pillai, V.B., Sundaresan, N.R., Samant, S.A., Wolfgeher, D., Trivedi, C.M., Gupta, M.P. (2011) Acetylation of a conserved lysine residue in the ATP binding pocket of p38 augments its kinase activity during hypertrophy of cardiomyocytes. *Mol. Cell. Biol.* **31,** 2349-2363

37. Sabo, A., Lusic, M., Cereseto, A., Giacca, M. (2008) Acetylation of conserved lysines in the catalytic core of cyclin-dependent kinase 9 inhibits kinase activity and regulates transcription. *Mol. Cell. Biol.* **28,** 2201-2212

38. Sundaresan, N.R., Pillai, V.B., Wolfgeher, D., Samant, S., Vasudevan, P., Parekh, V., Raghuraman, H., Cunningham, J.M., Gupta, M., Gupta, M.P. (2011) The deacetylase SIRT1 promotes membrane localization and activation of Akt and PDK1 during tumorigenesis and cardiac hypertrophy. *Sci. Signal.* **4,** ra46

39. Gerhart-Hines, Z., Dominy, J.E., Jr., Blattler, S.M., Jedrychowski, M.P., Banks, A.S., Lim, J.H., Chim, H., Gygi, S.P., Puigserver, P. (2011) The cAMP/PKA pathway rapidly activates SIRT1 to promote fatty acid oxidation independently of changes in NAD(+). *Mol. Cell* **44,** 851-863

40. Liu, Y., Denlinger, C.E., Rundall, B.K., Smith, P.W., Jones, D.R. (2006) Suberoylanilide hydroxamic acid induces Akt-mediated phosphorylation of p300, which promotes acetylation and transcriptional activation of RelA/p65. *J. Biol. Chem.* **281,** 31359-31368

41. Nasrin, N., Kaushik, V.K., Fortier, E., Wall, D., Pearson, K.J., de Cabo, R., Bordone, L. (2009) JNK1 phosphorylates SIRT1 and promotes its enzymatic activity. *PLoS One* **4,** e8414

42. Pflum, M.K., Tong, J.K., Lane, W.S., Schreiber, S.L. (2001) Histone deacetylase 1 phosphorylation promotes enzymatic activity and complex formation. *J. Biol. Chem.* **276,** 47733-47741

43. van Noort, V., Seebacher, J., Bader, S., Mohammed, S., Vonkova, I., Betts, M.J., Kuhner, S., Kumar, R., Maier, T., O'Flaherty, M., Rybin, V., Schmeisky, A., Yus, E., Stulke, J., Serrano, L., Russell, R.B., Heck, A.J., Bork, P., Gavin, A.C. (2012) Cross-talk between phosphorylation and lysine acetylation in a genome-reduced bacterium. *Mol. Syst. Biol.* **8,** 571

44. Yao, Q., Li, H., Liu, B.Q., Huang, X.Y., Guo, L. (2011) SUMOylation-regulated protein phosphorylation, evidence from quantitative phosphoproteomics analyses. *J. Biol. Chem.* **286,** 27342-27349

45. Paolinelli, R., Mendoza-Maldonado, R., Cereseto, A., Giacca, M. (2009) Acetylation by GCN5 regulates CDC6 phosphorylation in the S phase of the cell cycle. *Nat. Struct. Mol. Biol.* **16,** 412-420

46. Zhang, T., Wang, S., Lin, Y., Xu, W., Ye, D., Xiong, Y., Zhao, S., Guan, K.L. (2012) Acetylation negatively regulates glycogen phosphorylase by recruiting protein phosphatase 1. *Cell Metab.* **15,** 75-87

47. Govind, C.K., Qiu, H., Ginsburg, D.S., Ruan, C., Hofmeyer, K., Hu, C., Swaminathan, V., Workman, J.L., Li, B., Hinnebusch, A.G. (2010) Phosphorylated Pol II CTD recruits multiple HDACs, including Rpd3C(S), for methylation-dependent deacetylation of ORF nucleosomes. *Mol. Cell* **39,** 234-246

48. Ho, P.C., Gupta, P., Tsui, Y.C., Ha, S.G., Huq, M., Wei, L.N. (2008) Modulation of lysine acetylation-stimulated repressive activity by Erk2-mediated phosphorylation of RIP140 in adipocyte differentiation. *Cell Signal.* **20,** 1911-1919

49. Xiong, S., Salazar, G., San Martin, A., Ahmad, M., Patrushev, N., Hilenski, L., Nazarewicz, R.R., Ma, M., Ushio-Fukai, M., Alexander, R.W. (2010) PGC-1 alpha serine 570 phosphorylation and GCN5-mediated acetylation by angiotensin II drive catalase down-regulation and vascular hypertrophy. *J. Biol. Chem.* **285,** 2474-2487

50. Matsuzaki, H., Daitoku, H., Hatta, M., Aoyama, H., Yoshimochi, K., Fukamizu, A. (2005) Acetylation of Foxo1 alters its DNA-binding ability and sensitivity to phosphorylation. *Proc. Natl. Acad. Sci. U S A* **102,** 11278-11283

51. Mukherjee, S., Keitany, G., Li, Y., Wang, Y., Ball, H.L., Goldsmith, E.J., Orth, K. (2006) Yersinia YopJ acetylates and inhibits kinase activation by blocking phosphorylation. *Science* **312,** 1211-1214

52. Chou, T.Y., Hart, G.W., Dang, C.V. (1995) c-Myc is glycosylated at threonine 58, a known phosphorylation site and a mutational hot spot in lymphomas. *J. Biol. Chem.* **270,** 18961-18965

53. Musicki, B., Kramer, M.F., Becker, R.E., Burnett, A.L. (2005) Inactivation of phosphorylated endothelial nitric oxide synthase (Ser-1177) by O-GlcNAc in diabetes-associated erectile dysfunction. *Proc. Natl. Acad. Sci. U S A* **102,** 11870-11875

54. Kawauchi, K., Araki, K., Tobiume, K., Tanaka, N. (2009) Loss of p53 enhances catalytic activity of IKKbeta through O-linked beta-N-acetyl glucosamine modification. *Proc. Natl. Acad. Sci. U S A* **106,** 3431-3436

55. Bodenmiller, B., Wanka, S., Kraft, C., Urban, J., Campbell, D., Pedrioli, P.G., Gerrits, B., Picotti, P., Lam, H., Vitek, O., Brusniak, M.Y., Roschitzki, B., Zhang, C., Shokat, K.M., Schlapbach, R., Colman-Lerner, A., Nolan, G.P., Nesvizhskii, A.I., Peter, M., Loewith, R. et al (2010) Phosphoproteomic analysis reveals interconnected system-wide responses to perturbations of kinases and phosphatases in yeast. *Sci. Signal.* **3,** rs4

56. Holt, L.J., Tuch, B.B., Villen, J., Johnson, A.D., Gygi, S.P., Morgan, D.O. (2009) Global analysis of Cdk1 substrate phosphorylation sites provides insights into evolution. *Science* **325,** 1682-1686

57. Olsen, J.V., Vermeulen, M., Santamaria, A., Kumar, C., Miller, M.L., Jensen, L.J., Gnad, F., Cox, J., Jensen, T.S., Nigg, E.A., Brunak, S., Mann, M. (2010) Quantitative phosphoproteomics reveals widespread full phosphorylation site occupancy during mitosis. *Sci. Signal.* **3,** ra3

58. Choudhary, C., Kumar, C., Gnad, F., Nielsen, M.L., Rehman, M., Walther, T.C., Olsen, J.V., Mann, M. (2009) Lysine acetylation targets protein complexes and co-regulates major cellular functions. *Science* **325,** 834-840

59. Kim, S.C., Sprung, R., Chen, Y., Xu, Y., Ball, H., Pei, J., Cheng, T., Kho, Y., Xiao, H., Xiao, L., Grishin, N.V., White, M., Yang, X.J., Zhao, Y. (2006) Substrate and functional diversity of lysine acetylation revealed by a proteomics survey. *Mol. Cell* **23,** 607-618

60. Lundby, A., Lage, K., Weinert, B.T., Bekker-Jensen, D.B., Secher, A., Skovgaard, T., Kelstrup, C.D., Dmytriyev, A., Choudhary, C., Lundby, C., Olsen, J.V. (2012) Proteomic analysis of lysine acetylation sites in rat tissues reveals organ specificity and subcellular patterns. *Cell Rep.* **2,** 419-431

61. Wang, Q., Zhang, Y., Yang, C., Xiong, H., Lin, Y., Yao, J., Li, H., Xie, L., Zhao, W., Yao, Y., Ning, Z.B., Zeng, R., Xiong, Y., Guan, K.L., Zhao, S., Zhao, G.P. (2010) Acetylation of metabolic enzymes coordinates carbon source utilization and metabolic flux. *Science* **327,** 1004-1007

62. Weinert, B.T., Wagner, S.A., Horn, H., Henriksen, P., Liu, W.R., Olsen, J.V., Jensen, L.J., Choudhary, C. (2011) Proteome-wide mapping of the Drosophila acetylome demonstrates a high degree of conservation of lysine acetylation. *Sci. Signal.* **4,** ra48

63. Zhao, S., Xu, W., Jiang, W., Yu, W., Lin, Y., Zhang, T., Yao, J., Zhou, L., Zeng, Y., Li, H., Li, Y., Shi, J., An, W., Hancock, S.M., He, F., Qin, L., Chin, J., Yang, P., Chen, X., Lei, Q. et al (2010) Regulation of cellular metabolism by protein lysine acetylation. *Science* **327,** 1000-1004

64. Parker, B.L., Palmisano, G., Edwards, A.V., White, M.Y., Engholm-Keller, K., Lee, A., Scott, N.E., Kolarich, D., Hambly, B.D., Packer, N.H., Larsen, M.R., Cordwell, S.J. (2011) Quantitative N-linked glycoproteomics of myocardial ischemia and reperfusion injury reveals early remodeling in the extracellular environment. *Mol. Cell. Proteomics* **10,** M110 006833

65. Larsen, M.R., Thingholm, T.E., Jensen, O.N., Roepstorff, P., Jorgensen, T.J. (2005) Highly selective enrichment of phosphorylated peptides from peptide mixtures using titanium dioxide microcolumns. *Mol. Cell. Proteomics* **4,** 873-886

66. Engholm-Keller, K., Birck, P., Storling, J., Pociot, F., Mandrup-Poulsen, T., Larsen, M.R. (2012) TiSH - a robust and sensitive global phosphoproteomics strategy employing a combination of TiO(2), SIMAC, and HILIC. *J. Proteomics* **75,** 5749-5761

67. Yanes, O., Tautenhahn, R., Patti, G.J., Siuzdak, G. (2011) Expanding coverage of the metabolome for global metabolite profiling. *Anal. Chem.* **83,** 2152-2161

68. Hirao, M., Posakony, J., Nelson, M., Hruby, H., Jung, M.F., Simon, J.A., Bedalov, A. (2003) Identification of selective inhibitors of NAD(+)-dependent deacetylases using phenotypic screens in yeast. *J. Biol. Chem.* **278,** 52773-52782

69. Kall, L., Canterbury, J.D., Weston, J., Noble, W.S., MacCoss, M.J. (2007) Semi-supervised learning for peptide identification from shotgun proteomics datasets. *Nat. Methods* **4,** 923-925

70. Taus, T., Kocher, T., Pichler, P., Paschke, C., Schmidt, A., Henrich, C., Mechtler, K. (2011) Universal and confident phosphorylation site localization using phosphoRS. *J. Proteome Res.* **10,** 5354-5362

71. Karp, N.A., Huber, W., Sadowski, P.G., Charles, P.D., Hester, S.V., Lilley, K.S. (2010) Addressing accuracy and precision issues in iTRAQ quantitation. *Mol. Cell. Proteomics* **9,** 1885-1897

72. Toedling, J., Skylar, O., Krueger, T., Fischer, J.J., Sperling, S., Huber, W. (2007) Ringo--an R/Bioconductor package for analyzing ChIP-chip readouts. *BMC Bioinformatics* **8,** 221

73. Benjamini, Y., Hochberg, Y. (1995) Controlling the False Discovery Rate - a Practical and Powerful Approach to Multiple Testing. *J. Roy. Stat. Soc. B Met.* **57,** 289-300

74. Rigbolt, K.T., Vanselow, J.T., Blagoev, B. (2011) GProX, a user-friendly platform for bioinformatics analysis and visualization of quantitative proteomics data. *Mol. Cell. Proteomics* **10,** O110 007450

75. Obenauer, J.C., Cantley, L.C., Yaffe, M.B. (2003) Scansite 2.0: Proteome-wide prediction of cell signaling interactions using short sequence motifs. *Nucleic Acids Res.* **31,** 3635-3641

76. Shepherd, N.E., Hoang, H.N., Abbenante, G., Fairlie, D.P. (2005) Single turn peptide alpha helices with exceptional stability in water. *J. Am. Chem. Soc.* **127,** 2974-2983

77. Kubota, K., Anjum, R., Yu, Y., Kunz, R.C., Andersen, J.N., Kraus, M., Keilhack, H., Nagashima, K., Krauss, S., Paweletz, C., Hendrickson, R.C., Feldman, A.S., Wu, C.L., Rush, J., Villen, J., Gygi, S.P. (2009) Sensitive multiplexed analysis of kinase activities and activity-based kinase identification. *Nat. Biotechnol* **27,** 933-940

78. Yu, Y., Anjum, R., Kubota, K., Rush, J., Villen, J., Gygi, S.P. (2009) A site-specific, multiplexed kinase activity assay using stable-isotope dilution and high-resolution mass spectrometry. *Proc. Natl. Acad. Sci. U S A* **106,** 11606-11611

79. MacLean, B., Tomazela, D.M., Shulman, N., Chambers, M., Finney, G.L., Frewen, B., Kern, R., Tabb, D.L., Liebler, D.C., MacCoss, M.J. (2010) Skyline: an open source document editor for creating and analyzing targeted proteomics experiments. *Bioinformatics* **26,** 966-968

80. MacLean, B., Tomazela, D.M., Abbatiello, S.E., Zhang, S., Whiteaker, J.R., Paulovich, A.G., Carr, S.A., MacCoss, M.J. (2010a) Effect of collision energy optimization on the measurement of peptides by selected reaction monitoring (SRM) mass spectrometry. *Anal. Chem.* **82,** 10116-10124

81. Martin, D.B., Vagelos, P.R. (1962) The mechanism of tricarboxylic acid cycle regulation of fatty acid synthesis. *J. Biol. Chem.* **237,** 1787-1792

82. Ping, P., Zhang, J., Cao, X., Li, R.C., Kong, D., Tang, X.L., Qiu, Y., Manchikalapudi, S., Auchampach, J.A., Black, R.G., Bolli, R. (1999) PKC-dependent activation of p44/p42 MAPKs during myocardial ischemia-reperfusion in conscious rabbits. *Am. J. Physiol.* **276**, H1468-1481

83. Kirchberger, M.A., Tada, M., Repke, D.I., Katz, A.M. (1972) Cyclic adenosine 3',5'-monophosphate-dependent protein kinase stimulation of calcium uptake by canine cardiac microsomes. *J. Mol. Cell. Cardiol.* **4,** 673-680

84. Simmerman, H.K., Collins, J.H., Theibert, J.L., Wegener, A.D., Jones, L.R. (1986) Sequence analysis of phospholamban. Identification of phosphorylation sites and two major structural domains. *J. Biol. Chem.* **261,** 13333-13341

85. Bedalov, A., Gatbonton, T., Irvine, W.P., Gottschling, D.E., Simon, J.A. (2001) Identification of a small molecule inhibitor of Sir2p. *Proc. Natl. Acad. Sci. U S A* **98,** 15113-15118

86. Hebert, A.S., Dittenhafer-Reed, K.E., Yu, W., Bailey, D.J., Selen, E.S., Boersma, M.D., Carson, J.J., Tonelli, M., Balloon, A.J., Higbee, A.J., Westphall, M.S., Pagliarini, D.J., Prolla, T.A., Assadi-Porter, F., Roy, S., Denu, J.M., Coon, J.J. (2013) Calorie restriction and SIRT3 trigger global reprogramming of the mitochondrial protein acetylome. *Mol. Cell* **49,** 186-199

87. Baines, C.P., Zhang, J., Wang, G.W., Zheng, Y.T., Xiu, J.X., Cardwell, E.M., Bolli, R., Ping, P. (2002) Mitochondrial PKCepsilon and MAPK form signaling modules in the murine heart: enhanced mitochondrial PKCepsilon-MAPK interactions and differential MAPK activation in PKCepsilon-induced cardioprotection. *Circ. Res*. **90**, 390-397.

88. Hausenloy, D.J., Yellon, D.M. (2004) New directions for protecting the heart against ischemia-reperfusion injury: targeting the reperfusion injury salvage kinase (RISK)- pathway. *Cardiovasc. Res*. **61**, 448-460.

89. Beutner, G., Ruck, A., Riede, B., Brdiczka, D. (1998) Complexes between porin, hexokinase, mitochondrial creatine kinase and adenylate translocator display properties of the permeability transition pore. Implication for regulation of permeability transition by the kinases. *Biochim. Biophys. Acta* **1368,** 7-18

90. Broekemeier, K.M., Dempsey, M.E., Pfeiffer, D.R. (1989) Cyclosporin A is a potent inhibitor of the inner membrane permeability transition in liver mitochondria. *J. Biol. Chem.* **264,** 7826-7830

91. Pavlov, E.V., Priault, M., Pietkiewicz, D., Cheng, E.H., Antonsson, B., Manon, S., Korsmeyer, S.J., Mannella, C.A., Kinnally, K.W. (2001) A novel, high conductance channel of mitochondria linked to apoptosis in mammalian cells and Bax expression in yeast. *J. Cell Biol.* **155,** 725-731

92. Baines, C.P., Kaiser, R.A., Sheiko, T., Craigen, W.J., Molkentin, J.D. (2007) Voltage-dependent anion channels are dispensable for mitochondrial-dependent cell death. *Nat. Cell Biol.* **9,** 550-555

93. Kokoszka, J.E., Waymire, K.G., Levy, S.E., Sligh, J.E., Cai, J., Jones, D.P., MacGregor, G.R., Wallace, D.C. (2004) The ADP/ATP translocator is not essential for the mitochondrial permeability transition pore. *Nature* **427,** 461-465

94. Giorgio, V., von Stockum, S., Antoniel, M., Fabbro, A., Fogolari, F., Forte, M., Glick, G.D., Petronilli, V., Zoratti, M., Szabó, I., Lippe, G., Bernardi, P. (2013) Dimers of mitochondrial ATP synthase form the permeability transition pore. *Proc. Natl. Acad. Sci. USA* **110,** 5887-5892.

95. Sodi-Pallares, D., Testelli, M.R., Fishleder, B.L., Bisteni, A., Medrano, G.A., Friedland, C., De Micheli, A. (1962) Effects of an intravenous infusion of a potassium-glucose-insulin solution on the electrocardiographic signs of myocardial infarction. A preliminary clinical report. *Am. J. Cardiol.* **9,** 166-181

96. Kantor, P.F., Lucien, A., Kozak, R., Lopaschuk, G.D. (2000) The antianginal drug trimetazidine shifts cardiac energy metabolism from fatty acid oxidation to glucose oxidation by inhibiting mitochondrial long-chain 3-ketoacyl coenzyme A thiolase. *Circ. Res.* **86,** 580-588

97. Carr, S.M., Munro, S., Kessler, B., Oppermann, U., La Thangue, N.B. (2011) Interplay between lysine methylation and Cdk phosphorylation in growth control by the retinoblastoma protein. *EMBO J.* **30,** 317-327

98. Esteve, P.O., Chang, Y., Samaranayake, M., Upadhyay, A.K., Horton, J.R., Feehery, G.R., Cheng, X., Pradhan, S. (2011) A methylation and phosphorylation switch between an adjacent lysine and serine determines human DNMT1 stability. *Nat. Struct. Mol. Biol.* **18,** 42-48

99. Guo, Z., Zheng, L., Xu, H., Dai, H., Zhou, M., Pascua, M.R., Chen, Q.M., Shen, B. (2010) Methylation of FEN1 suppresses nearby phosphorylation and facilitates PCNA binding. *Nat. Chem. Biol.* **6,** 766-773

100. Sakamaki, J., Daitoku, H., Ueno, K., Hagiwara, A., Yamagata, K., Fukamizu, A. (2011) Arginine methylation of BCL-2 antagonist of cell death (BAD) counteracts its phosphorylation and inactivation by Akt. *Proc. Natl. Acad. Sci. U S A* **108,** 6085-6090

101. Yamagata, K., Daitoku, H., Takahashi, Y., Namiki, K., Hisatake, K., Kako, K., Mukai, H., Kasuya, Y., Fukamizu, A. (2008) Arginine methylation of FOXO transcription factors inhibits their phosphorylation by Akt. *Mol. Cell* **32,** 221-231

102. Cui, Y., Zhang, M., Pestell, R., Curran, E.M., Welshons, W.V., Fuqua, S.A. (2004) Phosphorylation of estrogen receptor alpha blocks its acetylation and regulates estrogen sensitivity. *Cancer Res.* **64,** 9199-9208

103. Rust, H.L., Thompson, P.R. (2011) Kinase consensus sequences: a breeding ground for crosstalk. *ACS Chem. Biol.* **6,** 881-892

104. Fischle, W., Wang, Y., Allis, C.D. (2003) Binary switches and modification cassettes in histone biology and beyond. *Nature* **425,** 475-479

Legends to Figures

Figure 1. Phosphorylation and lysine acetylation analysis from *ex vivo* myocardial tissue. (A) Langendorff perfused hearts were subjected to 0 or 20 min ischemia or ischemic preconditioning (IPC) with or without the presence of 10 μM splitomicin during 20 min of baseline (non-ischemic) perfusion. Quantification was performed by TMT isobaric labeling and sequential enrichment of lysine acetylated peptides and phosphopeptides. Peptides were fractionated with HILIC and analyzed by reversed phase nLC-MS/MS. **(B)** Histograms showing the distribution of phosphopeptides (purple; phospho), lysine acetylated peptides (blue; AcetylK) and total protein (orange) quantification expressed as Log_2 ratios relative to 0 min ischemia (0i).

Figure 2. Site-specific relative quantification of modified peptides and total protein (A) and metabolites (B) from pathways highlighted in ischemia and ischemic preconditioning (IPC), in the presence or absence of splitomicin. (A) Relative quantification (heat maps) of phosphopeptides (side bar - purple; phospho), lysine acetylated peptides (side bar - blue; AcetylK) and total protein (side bar - orange) with quantification expressed as Log_2 ratios relative to 0 min ischemia (0i) for selected proteins clustered into the pathways 'fatty acid metabolism', 'TCA cycle' and 'glycolysis'. (B) Selected metabolites quantified by LC-SRM; ** p <0.001; * p<0.05; F-1,6-B, fructose 1,6-bisphosphate.

Figure 3. Kinase activation during myocardial ischemia is regulated by splitomicin-mediated inhibition of SIRT1-associated lysine deacetylation. (**A**) Fuzzy c-means clustering of phosphopeptides differentially regulated between 0 min ischemia (0i) (or 0 min ischemia with splitomicin (0iSPLIT)) and 20 min ischemia (20i) but not attenuated following 20 min ischemia in the presence of splitomicin. (**B**) Fuzzy c-means clustering of phosphopeptides differentially regulated between 0 min ischemia (0i) (or 0 min ischemia with splitomicin (0iSPLIT)) and 20 min ischemia (20i), and attenuated by 20 min ischemia with splitomicin (20iSPLIT). (**C**) Site-specific analysis of phosphopeptides (>75% localization probability) clustered in (**B**) regulated by 20i and attenuated with splitomicin. Previously verified targets of AMPK (green), AKT (purple) and PKA (blue) with ischemia-induced increases in phosphorylation attenuated by splitomicin (Table S1). **(D)** Immunoblotting shows splitomicin attenuates ischemia-associated phosphorylation of: Thr-172 AMPKα, Ser-473 AKT, Ser-422 eIF4B, Ser-79 ACC, (**E**) PKA substrate; relative to 0 min ischemia and 20 min normoxic time control perfusion (TC). Blots are representative of n=3. (**F,G**) Relative quantification of Acetyl-CoA **(F)** and cAMP **(G)** by LC-SRM in myocardial tissue subjected to 20 min ischemia (20i) or 20 min ischemia with splitomicin (20iSPLIT) expressed relative to 0 min ischemia (0i) (n=3). * p-value < 0.05 (two-side t-test). Error bars show standard deviation.

Figure 4. *In vitro* kinase and phosphatase assays demonstrate the kinetic effects of proximal phosphorylation and AcetylK on the CKM peptide ^{364}EKKLEKGQSIDD^{375}: i) non-modified (KxxS); ii) phosphorylated at S9 (S372; KxxpS); iii) acetylated at K6 (K369; AcKxxS); iv) acetylated at K6 and phosphorylated at S9 (K369 and S372; AcKxxpS); v) AcetylK mimic Q6 and phosphorylated at S9 (K369Q and S372; QxxpS) and; vi) AcetylK negative R6 and phosphorylated at S9 (K369R and S372; RxxpS). (**A**) Kinase assay using KxxS and AcKxxS spiked separately into lysates in the presence of phosphatase and deacetylase inhibitors. (**B**) Phosphatase assay using KxxpS and AcKxxpS spiked separately into lysates in the absence of phosphatase and deacetylase inhibitors. (**C**) Phosphatase assay using KxxpS and AcKxxpS spiked separately into lysates in the presence of phosphatase and deacetylase inhibitors. (**D**) Phosphatase assay using QxxpS and RxxpS spiked separately into lysates in the absence of phosphatase deacetylase inhibitors. (**E**) Kinase assay using KxxS and AcKxxS with purified recombinant CaMKII. (**F**) Phosphatase assay using KxxpS and AcKxxpS with purified recombinant antarctic phosphatase. (**G**) Phosphatase assay using QxxpS and RxxpS with purified recombinant antarctic phosphatase. Peak areas of all variants were simultaneously monitored for each reaction using nLC-SRM to obtain % substrate conversion [$Area_{product}/(Area_{substrate} + Area_{product})$] at 0, 10, 20, 30 and 60 min (n=3).

Figure 5. *In vitro* phosphatase and deacetylase assays using SILAC labelled, immunoprecipitated full-length CKM wild-type (WT), AcetylK mimic (K369Q) and phospho-mimic (S372E). (**A**) **and (C**) Overview of the approach. FLAG-tagged WT, K369Q (A) and S372E (C) CKM were over-expressed in light (L) and heavy (H) SILAC labelled rat L6 myoblasts. Following immunopreciptation, CKM from both light and heavy labelled cells was subjected to: (A) an *in vitro* kinase assay with CaMKII. Heavy labelled CKM was subsequently subjected to phosphatase assays with protein phosphatase 1 (PP1) for 30 or 60 min; or (C) an *in vitro* deacetylase assay with immunoprecipitated FLAG-tagged SIRT1 for 30 or 60 min Light and heavy labelled CKM were eluted, mixed, digested and the rates of dephosphorylation or deacetylation measured between light and heavy labelled peptides using nLC-MS/MS. (**B**) Quantification of the relative abundance of the SILAC phosphopeptides GQSpIDDMIPAQK (WT) and KLEQGQSpIDDMIPAQK (K369Q) between light (untreated) and heavy (treated with PP1 for 30 or 60 min) showing the rate of dephosphorylation expressed as Log_2(H/L). (**D**) Quantification of the relative abundance of the SILAC acetylated peptide KLEK(Ac)GQSIDDMIPAQK (WT) and KLEK(Ac)GQEIDDMIPAQK (S372E) between light (untreated) and heavy (treated with SIRT1 for 30 or 60 min) showing the rate of deacetylation expressed as Log_2(H/L).

Figure 6. Analysis of CKM *C*-terminal peptide ^{364}EKKLE<u>KGQS</u>IDD^{375}: i) phosphorylated at S9 (S372; KxxpS) or ii) acetylated at K6 and phosphorylated at S9 (K369 and S372; AcKxxpS) by 2D ^{1}H NMR total correlation spectroscopy (TOCSY) and Nuclear Overhauser effect spectroscopy (NOESY). Overlays of (**A**) HA-HN TOCSY region of acetylated (AcKxxpS) and non-acetylated (KxxpS) phosphopeptide; (**B**) HB-HN TOCSY and NOESY region of the acetylated phosphopeptide (AcKxxpS); (**C**) side chain NOESY region of the acetylated (AcKxxpS) and non-acetylated (KxxpS) phosphopeptide. (**D**) Proposed conformation of the acetylated (AcKxxpS) and non-acetylated (KxxpS) phosphopeptide.

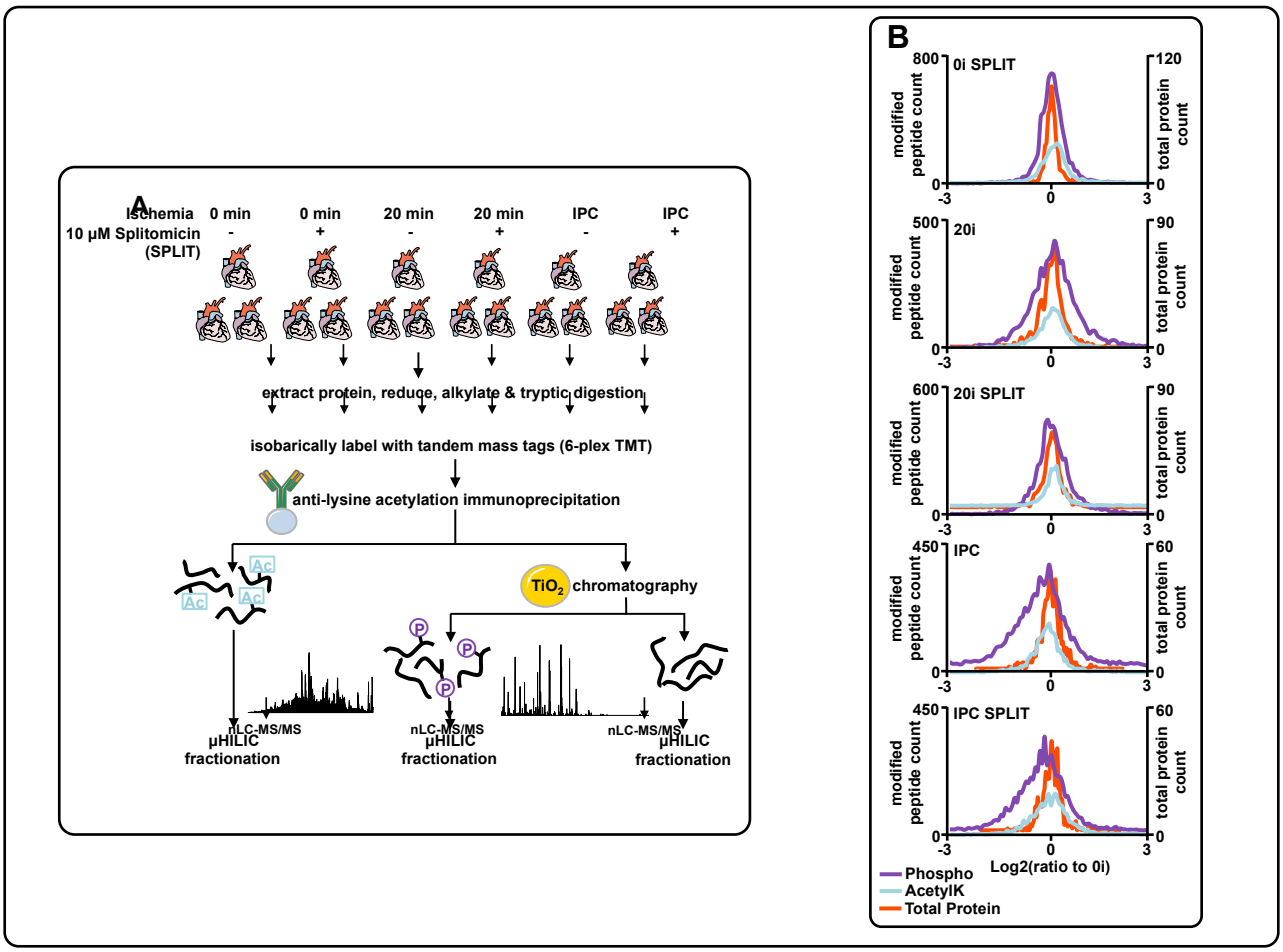
A
Ischemia
10 µM Splitomicin (SPLIT)
0 min -
0 min +
20 min -
20 min +
IPC -
IPC +
extract protein, reduce, alkylate & tryptic digestion
isobarically label with tandem mass tags (6-plex TMT)
anti-lysine acetylation immunoprecipitation
TiO2 chromatography
Ac
P
nLC-MS/MS
µHILIC fractionation
B
0i SPLIT
20i
20i SPLIT
IPC
IPC SPLIT
modified peptide count
total protein count
Log2(ratio to 0i)
Phospho
AcetylK
Total Protein

Figure 1.

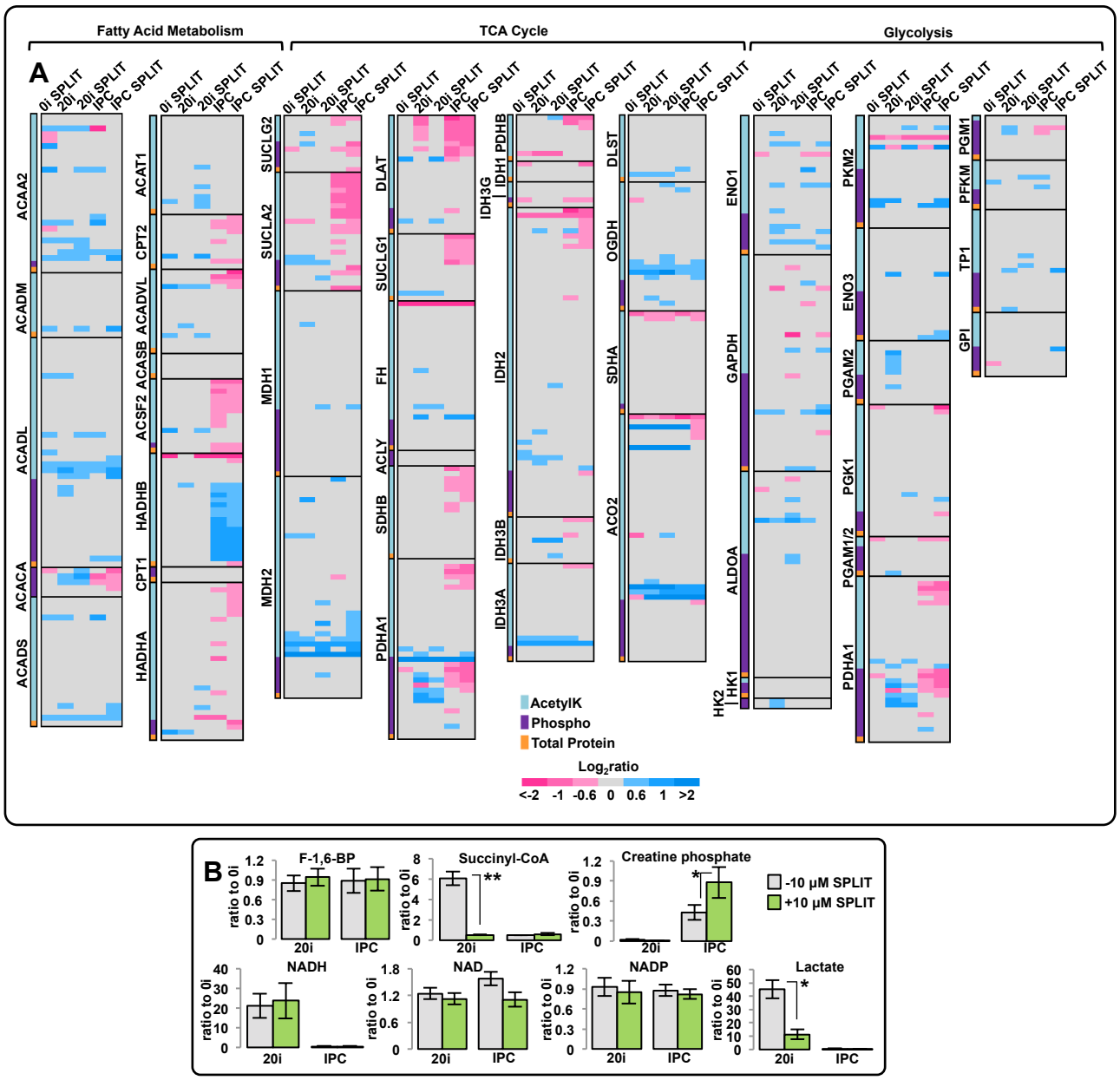
A
Fatty Acid Metabolism
TCA Cycle
Glycolysis
0i SPLIT
20i
20i SPLIT
IPC
IPC SPLIT
ACAA2
ACADM
ACADL
ACACA
ACADS
ACAT1
CPT2
ACADVL
ACASB
ACSF2
HADHB
CPT1
HADHA
SUCLG2
SUCLA2
MDH1
MDH2
DLAT
SUCLG1
FH
ACLY
SDHB
PDHA1
IDH3G
IDH1
PDHB
IDH2
IDH3B
IDH3A
DLST
OGDH
SDHA
ACO2
ENO1
GAPDH
ALDOA
HK2
HK1
PKM2
ENO3
PGAM2
PGK1
PGAM1/2
PDHA1
PGM1
PFKM
TP1
GPI
AcetylK
Phospho
Total Protein
Log2ratio
<-2 -1 -0.6 0 0.6 1 >2
B
F-1,6-BP
Succinyl-CoA
Creatine phosphate
NADH
NAD
NADP
Lactate
ratio to 0i
20i
IPC
-10 µM SPLIT
+10 µM SPLIT
**
*

Figure 2.

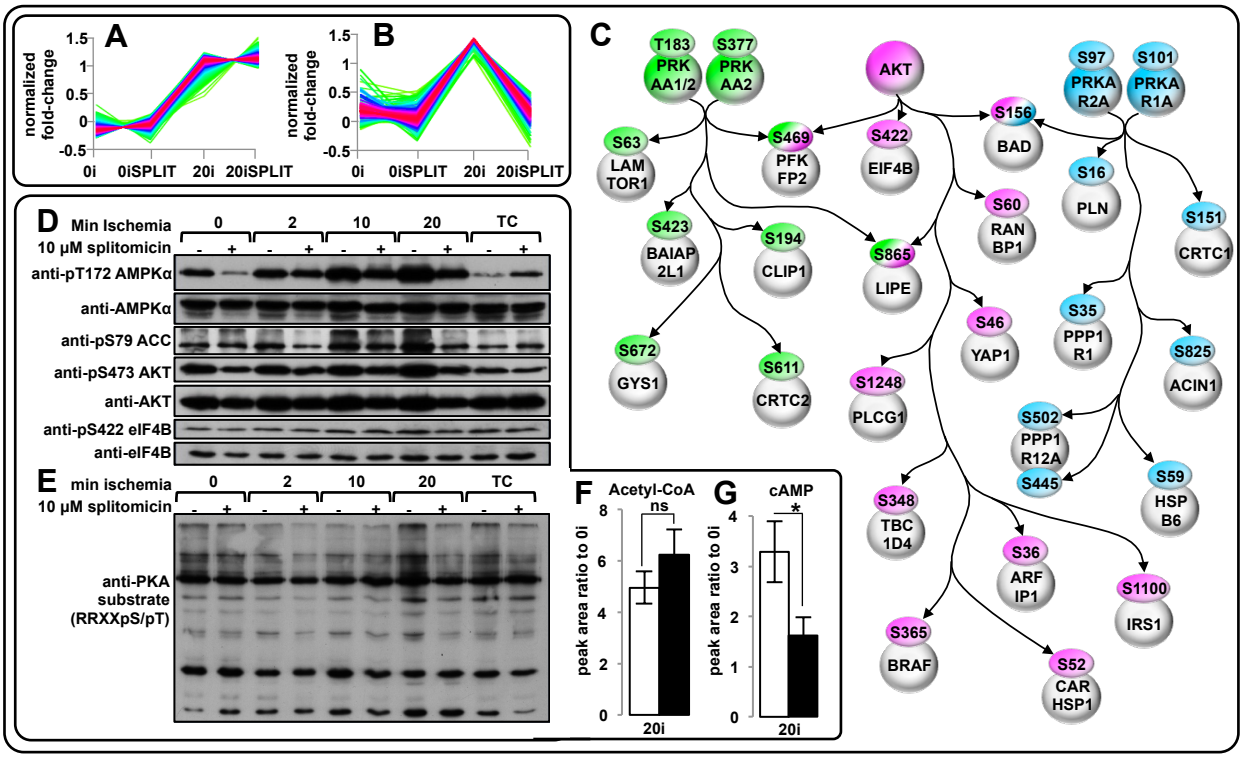
A
B
normalized fold-change
1.5
1
0.5
0
-0.5
0i
0iSPLIT
20i
20iSPLIT
C
T183 PRKAA1/2
S377 PRKAA2
AKT
S97 PRKAR2A
S101 PRKAR1A
S63 LAMTOR1
S469 PFKFP2
S422 EIF4B
S156 BAD
S16 PLN
S60 RANBP1
S151 CRTC1
S423 BAIAP2L1
S194 CLIP1
S865 LIPE
S46 YAP1
S35 PPP1R1
S672 GYS1
S611 CRTC2
S1248 PLCG1
S825 ACIN1
S502 PPP1R12A
S445
S59 HSPB6
S348 TBC1D4
S36 ARFIP1
S1100 IRS1
S365 BRAF
S52 CARHSP1
D
Min Ischemia
0
2
10
20
TC
10 μM splitomicin
anti-pT172 AMPKα
anti-AMPKα
anti-pS79 ACC
anti-pS473 AKT
anti-AKT
anti-pS422 eIF4B
anti-eIF4B
E
min ischemia
anti-PKA substrate (RRXXpS/pT)
F
Acetyl-CoA
ns
peak area ratio to 0i
8
6
4
2
0
20i
G
cAMP
*
peak area ratio to 0i
4
3
2
1
0
20i

Figure 3.

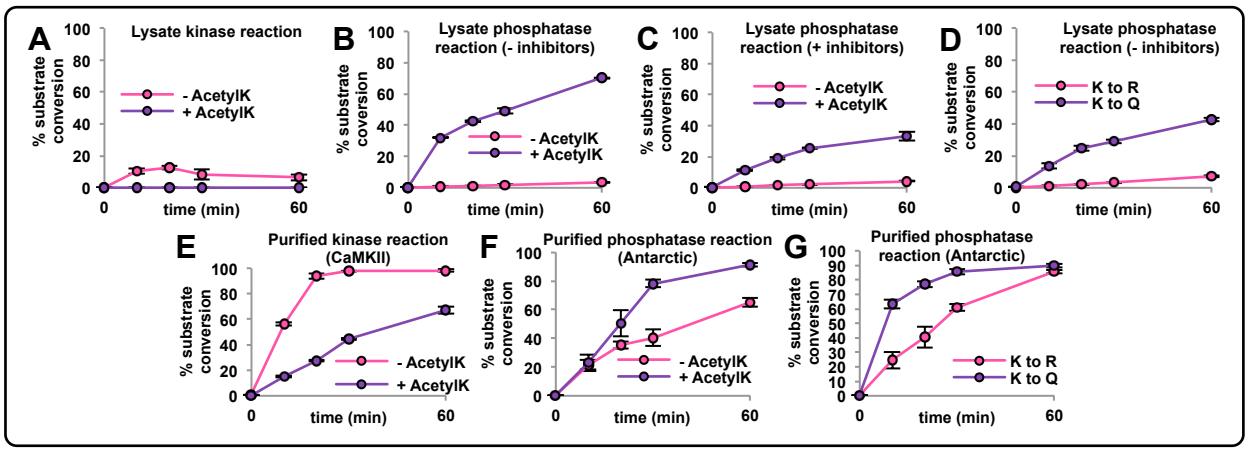
A
Lysate kinase reaction
% substrate conversion
- AcetylK
+ AcetylK
time (min)
B
Lysate phosphatase reaction (- inhibitors)
C
Lysate phosphatase reaction (+ inhibitors)
D
Lysate phosphatase reaction (- inhibitors)
K to R
K to Q
E
Purified kinase reaction (CaMKII)
F
Purified phosphatase reaction (Antarctic)
G
Purified phosphatase reaction (Antarctic)

Figure 4.

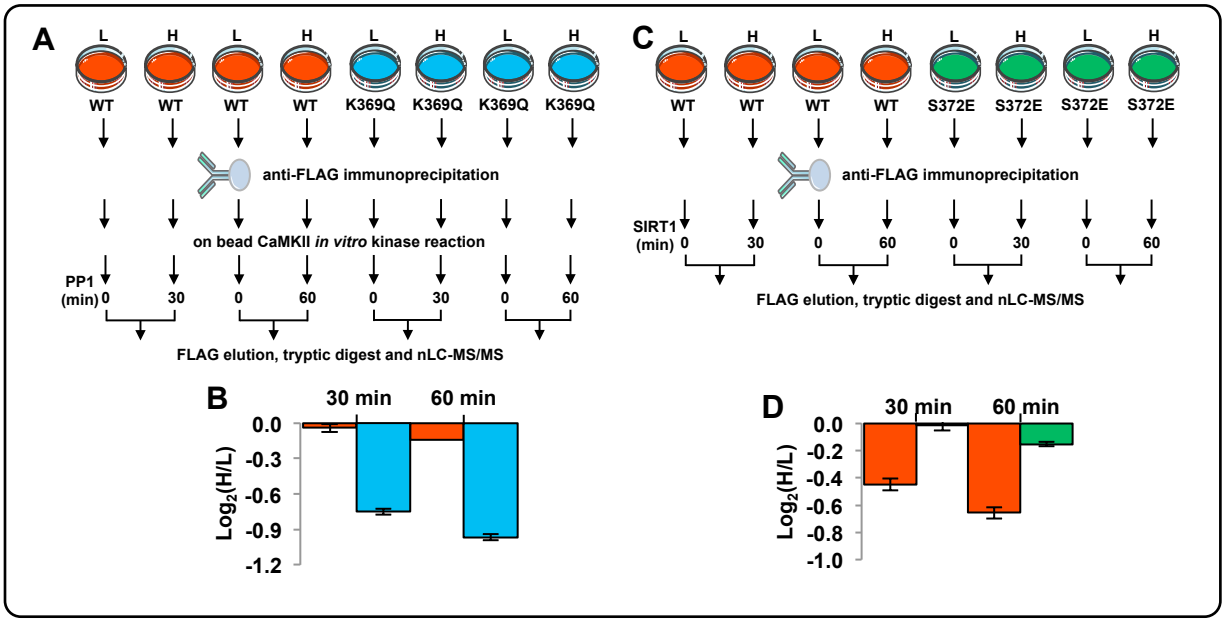
A
L H L H L H L H
WT WT WT WT K369Q K369Q K369Q K369Q
anti-FLAG immunoprecipitation
on bead CaMKII in vitro kinase reaction
PP1 (min) 0 30 0 60 0 30 0 60
FLAG elution, tryptic digest and nLC-MS/MS
C
L H L H L H L H
WT WT WT WT S372E S372E S372E S372E
anti-FLAG immunoprecipitation
SIRT1 (min) 0 30 0 60 0 30 0 60
FLAG elution, tryptic digest and nLC-MS/MS
B
30 min 60 min
Log2(H/L)
0.0 -0.3 -0.6 -0.9 -1.2
D
30 min 60 min
Log2(H/L)
0.0 -0.2 -0.4 -0.6 -0.8 -1.0

Figure 5.

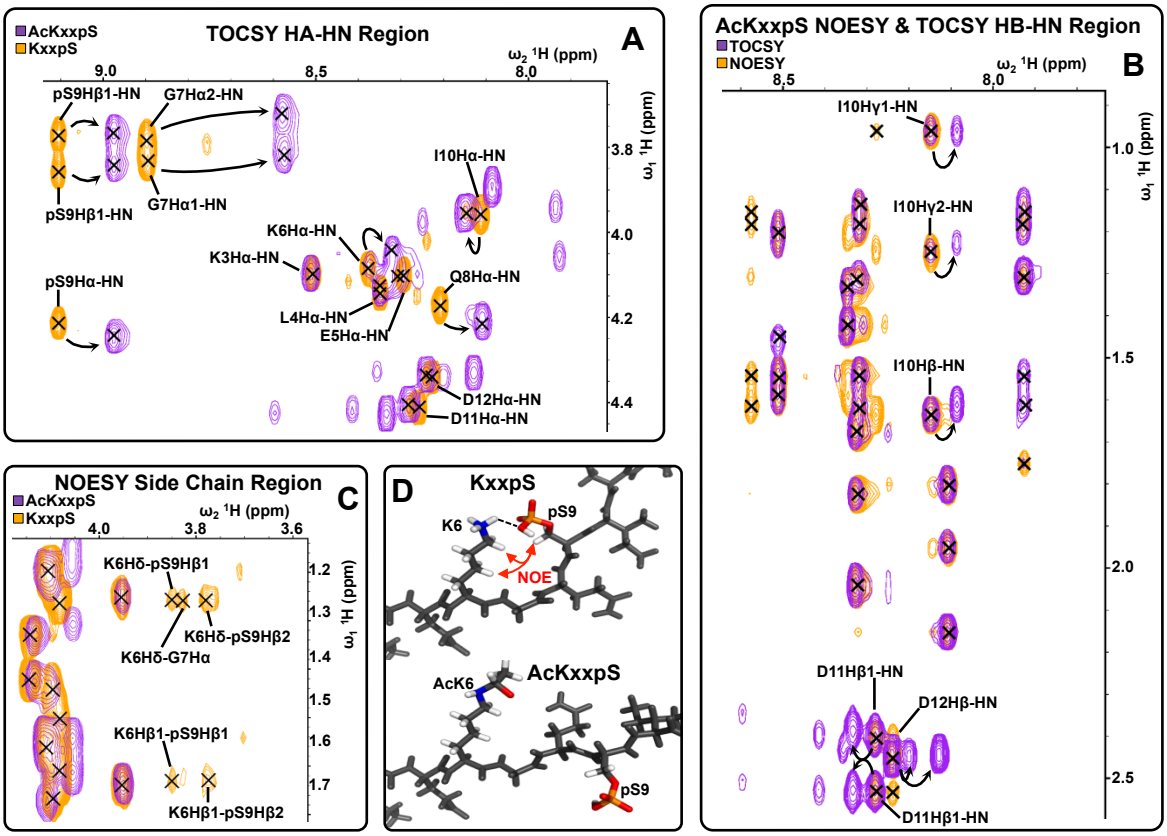
A
TOCSY HA-HN Region
AcKxxpS
KxxpS
ω2 1H (ppm)
9.0
8.5
8.0
ω1 1H (ppm)
3.8
4.0
4.2
4.4
pS9Hβ1-HN
G7Hα2-HN
pS9Hβ1-HN
G7Hα1-HN
I10Hα-HN
K6Hα-HN
K3Hα-HN
Q8Hα-HN
pS9Hα-HN
L4Hα-HN
E5Hα-HN
D12Hα-HN
D11Hα-HN
B
AcKxxpS NOESY & TOCSY HB-HN Region
TOCSY
NOESY
ω2 1H (ppm)
8.5
8.0
ω1 1H (ppm)
1.0
1.5
2.0
2.5
I10Hγ1-HN
I10Hγ2-HN
I10Hβ-HN
D11Hβ1-HN
D12Hβ-HN
D11Hβ1-HN
C
NOESY Side Chain Region
AcKxxpS
KxxpS
ω2 1H (ppm)
4.0
3.8
3.6
ω1 1H (ppm)
1.2
1.3
1.4
1.5
1.6
1.7
K6Hδ-pS9Hβ1
K6Hδ-pS9Hβ2
K6Hδ-G7Hα
K6Hβ1-pS9Hβ1
K6Hβ1-pS9Hβ2
D
KxxpS
K6
pS9
NOE
AcK6
AcKxxpS
pS9

Figure 6.